JOC The Journal of Organic Chemistry

Article

Pd-Catalyzed Carbonylation of Acyl Azides

Zongyang Li, Shiyang Xu, Baoliang Huang, Chenhui Yuan,
Wenxu Chang, Bin Fu, Lei Jiao, Peng Wang, and Zhenhua Zhang

J. Org. Chem., **Just Accepted Manuscript** • DOI: 10.1021/acs.joc.9b01048 • Publication Date (Web): 03 Jul 2019

Just Accepted

is published by the American Chemical Society. 1155 Sixteenth Street N.W., Washington, DC 20036

Pd-Catalyzed Carbonylation of Acyl Azides

Zongyang Li,† Shiyang Xu,† Baoliang Huang,† Chenhui Yuan,† Wenxu Chang,† Bin Fu,† Lei Jiao,‡, Peng Wang,† Zhenhua Zhang*,†*

† Beijing Advanced Innovation Center for Food Nutrition and Human Health, China Agricultural University, Beijing 100193, China and Department of Applied Chemistry, China Agricultural University, Beijing 100193, China

‡ Center of Basic Molecular Science (CBMS), Department of Chemistry, Tsinghua University, Beijing 10084, China

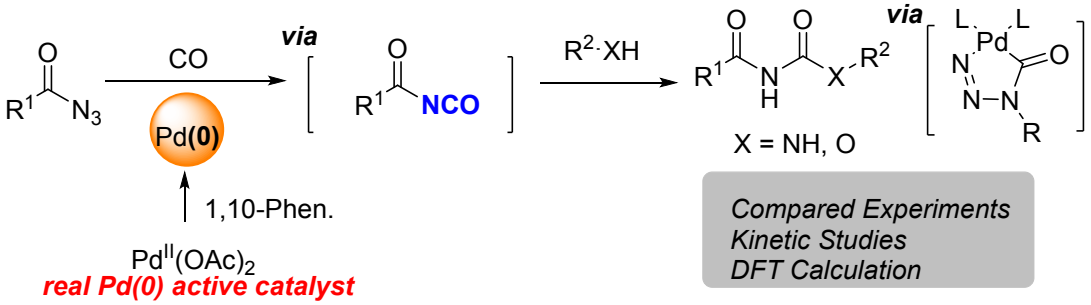

Key words: Acyl azide • Carbonylation • Mechanistic study • Five-membered palladacycle

ABSTRACT: Pd-catalyzed reactions of azides with CO to access isocynate intermediate have been developed extensively in recent years. However, the catalytic carbonylation of sensitive acyl azides has not been reported. Herein, we report a simple Pd-catalyzed carbonylation reaction of acyl azides with broad substrate scope, high efficiency, and simple operation under mild conditions, which provides facile access to acyl ureas. In addition, mechanistic study was carried out by both experiment and DFT calculation. Control experiments and kinetic study revealed that the real active palladium species were Pd(0). The result of kinetic study suggested that palladium catalyst, azide, and CO were all involved in the turnover-limiting step except amine. Further DFT study suggested that an unprecedented five-membered palladacycle intermediate was the key intermediate in the carbonylation reaction.

Introduction

Acyl urea derivatives are common motifs in pharmaceuticals and agrochemicals.[1] The traditional method for accessing acyl urea is the transformation of amides with phenyl carbamates, which produces stoichiometric phenol as a byproduct.[2] Other approaches involve the coupling of isocyanates with amides and acyl isocyanates with amines, both of which usually require the use of unfriendly phosgene.[3] Pd-catalyzed carbonylation has also been well-established as one of the most important ways to introduce C=O group into organic molecules.[4] Recently, simple Pd(II) salts catalyzed reaction of azides with σ-donor/π-acceptors, such as CO[5] and isocyanide[6], to form isocyanates and carbodiimides under mild

conditions received considerable attention from the synthetic community (Scheme 1a). Nevertheless, the catalytic carbonylation of sensitive acyl azides, which could easily undergo Curtius rearrangement, has not been achieved (Scheme 1b). Herein, we describe a Pd-catalyzed direct carbonylation of acyl azides with balloon-pressured CO, followed by one-pot reaction with amines at room temperature to afford acyl ureas with excellent yields (Scheme 1c). This reaction represents a novel and efficient access to urea derivatives, and the related mechanistic study revealed a new Pd(0)-initiated pathway, which has not been established in literature.

Scheme 1 The approach to synthesize acyl ureas

a). Pd(II) catalyzed carbonylation of azide

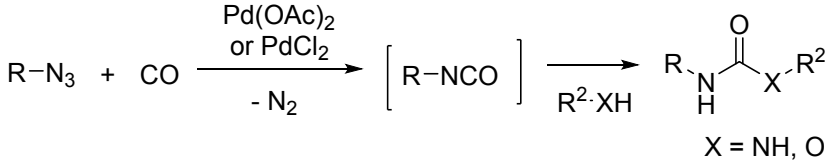

b). The traditional method of acyl urea synthesis

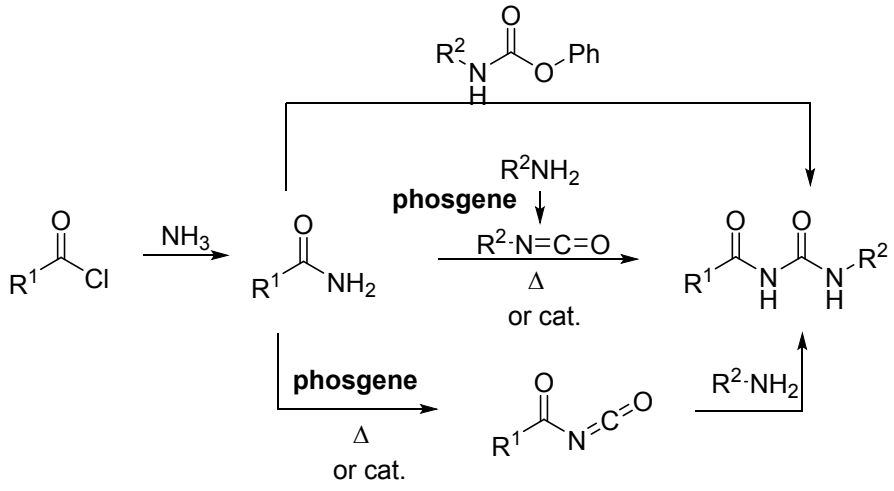

c). This work

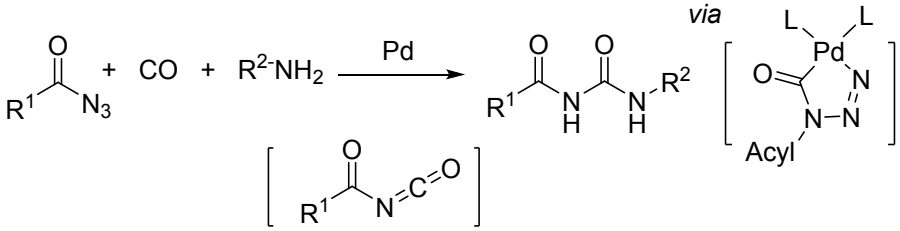

RESULTS AND DISCUSSION

Optimization of the Reaction Conditions. Initially, Pd-catalyzed carbonylative coupling reaction of benzoyl azide **1a** and 4-methoxyaniline **2a** was investigated as the model reaction (Table 1, *for more details, please see Table S1 of the Supporting Information*). We first carried out the model reaction with $Pd(OAc)_2$ as the catalyst without any external ligands, which showed no catalytic activity (entry 1). When 1,10-phen was added as the ligand, the reaction gave an excellent yield of 98% (entry 2). $PdCl_2$ with 1,10-phen ligand was found to be ineffective (entry 3). Once AcO^- was added, the yield varied between 77 to

98% (entry 4 and 5). Pd(0) catalysts were also proved active. When $Pd_2(dba)_3$, $Pd(dba)_2$, and $Pd(P^tBu_3)_2$ were used, the reaction gave 85%, 80%, and 83% yield respectively. However, $Pd_2(dba)_3$ alone showed no activity (entry 9). In addition, no reaction occurred if CO was replaced by N_2 (entry 10).

Table 1. Conditions of Pd-Catalyzed Reaction of Acyl Azide **1a** with CO and Anline **2a**.[a]

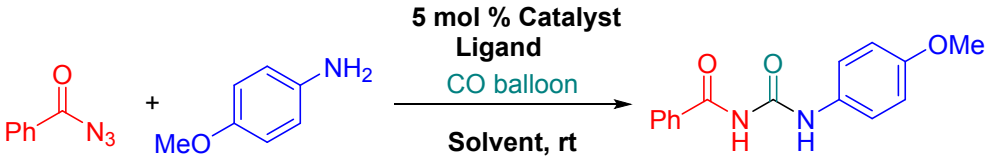

1a **2a** **3aa**

Entry	Catalyst	Ligand (mol %)	Yield[b] (%)
1	$Pd(OAc)_2$	--	nr
2	$Pd(OAc)_2$	1, 10-Phen (5)	98
3	$PdCl_2$	1, 10-Phen (5)	nr
4	$PdCl_2$	1, 10-Phen (5) / NaOAc(20)	98
5	$PdCl_2$	1, 10-Phen (5) / NH_4OAc(20)	77
6	$Pd_2(dba)_3$	1, 10-Phen (5)	85
7	$Pd(dba)_2$	1, 10-Phen (5)	80
8	$Pd(P^tBu_3)_2$	1, 10-Phen (5)	83
9	$Pd_2(dba)_3$	--	nr
10[c]	$Pd_2(dba)_3$	1, 10-Phen (5)	nr

a. Reaction condition: **1a** (0.20 mmol), **2a** (0.24 mmol), catalyst (5 mol %), ligand (5 mol %), CO (1 atm), solvent (3 mL), rt, 8 h. *b*. Isolated yield. "nr" = no reaction. 1,10-phen = 1,10-phenanthroline. *c*. N_2 instead of CO.

Substrate Scope. On the basis of the optimized condition, we expanded the scope of substrates to access a variety of potentially bioactive compounds (Scheme 2). We initially examined different substitutents including electron-withdrawing groups on the azide component such as $-CF_3$ (**3cb**) and electron-donating groups like -OMe (**3bb**). To our delight, both of them afforded excellent yields. Subsequently, various substituents on different positions of the acyl azide were investigated in this transformation. The results showed that *para*- (**3db**) and *meta*- (**3eb**) substituted products were formed in excellent yields, and *ortho*- (**3fb**) product also afforded good yield. We further expanded the substrate scope to halogen-substituted acyl azides (**3gb**, **3hb** and **3ib**). The corresponding products were obtained with excellent functional group tolerance except iodide (**3ib**, 50%). Moreover, 2-phenylacetyl azide and 3-phenylpropanoyl azide were employed as starting materials, giving 88% (**3ob**) and 65% (**3pb**) yields when 2,9-dimethyl-4,7-diphenyl-1,10-phenanthroline was used as the ligand. Furthermore, we successfully and efficiently formed products

bearing reactive functionalities, such as 4-CN (**3kb**), 4-CH=CH_2 (**3mb**), and 4-COOMe (**3jb**). Finally, naphthyl-ring (**3nb**), heterocyclic acyl azides (**3qb** – **3vb**) and aryl / benzyl azides (**3wb** and **3xb**) all furnished good yields.

Scheme 2. Substrate Scope of the Carbonylation Reaction of Acyl Azide [a]

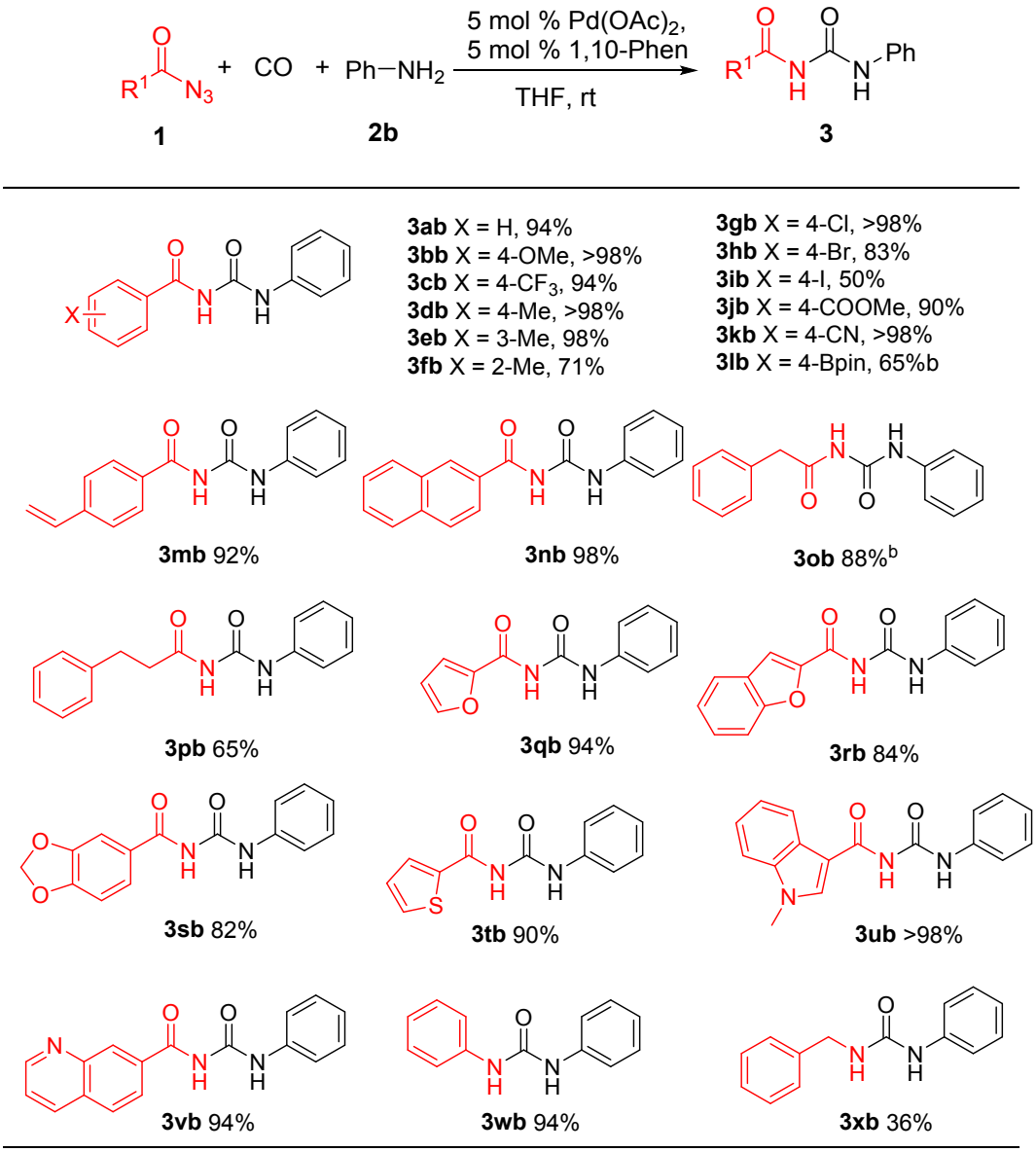

a. Reaction conditions: **1** (0.20 mmol), **2b** (0.24 mmol), $Pd(OAc)_2$ (5 mol %), 1,10-phen (5 mol %), CO (1 atm), THF (3 mL), rt, 12h, isolated yield; *b*. Using 2,9-dimethyl-4,7-diphenyl-1,10-phenanthroline as the ligand. *c*. **1d** (6.21 mmol), **2b** (7.45 mmol), $Pd(OAc)_2$ (5 mol %), 1,10-phen (5 mol %), CO (1 atm), THF (25 mL), rt, 12h, **3db** (1.55 g), 98% isolated yield.

On the other hand, various nucleophiles have also been investigated in this reaction (Scheme 3). First, we surveyed different substituted anilines, including electronic and positional variation of substituents. Yields of the corresponding desired products were good to quantitative (75-98%). For instance, in 4-CF_3

(**3ac**), 4-CN (**3al**), 4-OMe (**3aa**), and 4-Ph (**3am**)-substituted cases, both electron-withdrawing and electron-donating groups gave high yields. Anilines bearing substituents on different positions of the aromatic ring also gave the corresponding products with high yields. Besides, halogen (**3ag-3aj**), ester (**3an**) and boronic acid ester (**3ao**)-substituted products were obtained efficiently in good to excellent yields. Moreover, naphthylamine (**3ap**) and alkyl amines (**3aq-3ar**) produced the desired acylureas in moderate to good yields. In particular, ethanol as the nucleophile also demonstrated good reactivity (**3at**). Unfortunately, secondary amines failed to react, which might be attributed to the deactivation of the palladium catalyst caused by the enhanced coordinative ability of secondary amines.

Scheme 3 Substrate Scope of the Carbonylation Reaction of Amine [a]

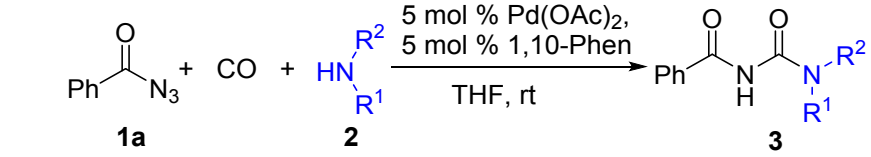

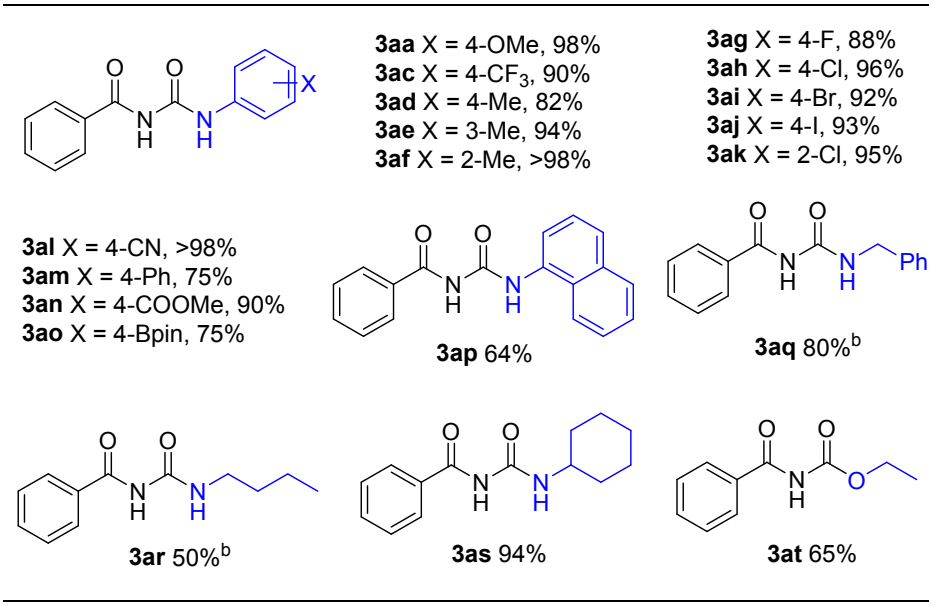

a. Reaction conditions: **1** (0.20 mmol), **2** (0.24 mmol), $Pd(OAc)_2$ (5 mol %), 1,10-phen (5 mol %), CO (1 atm), THF (3 mL), rt, 12h, isolated yield; *b*. Amine was added *via* syringe.

MECHANISTIC STUDY

Based on the reactions mentioned above, we found that both Pd(0) and Pd(II) could catalyze the carbonylation reaction of acyl azides. It has been established that in literature that the carbonylation of aryl azides could be initiated by Pd(II).[5b] In the study of our own research group, we also discovered that a sulfonylurea product-derived Pd(II) complex acted as the catalytically active species to interact with the sulfonylazide.[5d] In the study of Grushin research group, Pd(0)/Xantphos was found to catalyze the aromatic azidocarbonylation, and the aroyl azide products did not undergo further Pd-catalyzed carbonylation.[7] Therefore, the observation that Pd(0) species exhibited comparable catalytic activity to Pd(II) prompted us to investigate the reaction mechanism, in particular to figure out the real catalytic species and the pathway of azide activation and carbonylation.

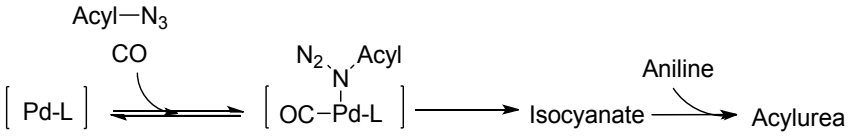

Kinetic Study: First we set out to study the kinetic behavior of reactants and catalyst in the catalytic cycle. The reaction between benzoyl azide (**1a**) and aniline (**2b**) employing catalytic $Pd(OAc)_2$/1,10-phen was selected as the model reaction for kinetic study. Because the reaction under study was rather rapid, we used relatively low concentrations (around 5 mM) of both **1a** and **2b** to reach a reasonable reaction rate. LC-MS method was utilized to perform the quantitative analysis of the reaction mixture.[8] The concentration of product **3ab** was followed versus time to detect the initial rate of the reaction, and the dependence of the initial rate on different reaction components was investigated.

It was observed that, in all kinetic profiles acquired there were a significant induction period (Figure 1a-d, ca. 2 min). The concentration of aniline (**2b**) had a minor effect on the initial rate of the reaction (Figure 1a). The concentration of Pd/Ligand and benzoyl azide (**1a**) both had positive effects on the reaction (Figure 1b-1c). The initial rate even exhibited first-order dependence on the concentrations of both Pd/L and **1a** (*for more details, please see Part 2.2 and 2.3 of the Supporting Information*). The dependence of initial rate on CO pressure was rather intriguing. Under a low CO pressure (using CO/N_2 mixture balloons with CO content varied from 50%, 66.7%, 80%, to 100%)[9], a positive dependence was observed (Figure 1d). However, under a higher CO pressure (2 atm), the reaction was inhibited and the starting material azide **1a** remained intact. These results illustrated that CO had a positive effect on the reaction under a low pressure, but a negative effect in under a high pressure.

Furthermore, Hammett analyses of different *para*-substituted anilines and benzoyl azides were performed by correlating $\ln(k_{rel})$ with σ^+.[10] For different *para*-substituted anilines, the slope of the linear correlation (ρ) was +0.021 (Figure 1e), also suggesting that the aniline component was not involved in the turnover-limiting step of the reaction. For different *para*-substituted benzoyl azides, ρ value of -0.305 was obtained, further implying that azide had a significant impact on the turnover-limiting step.

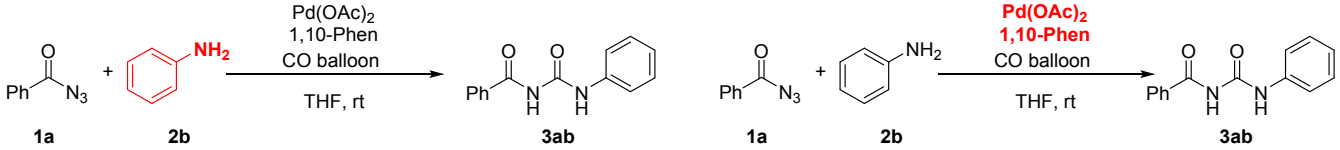

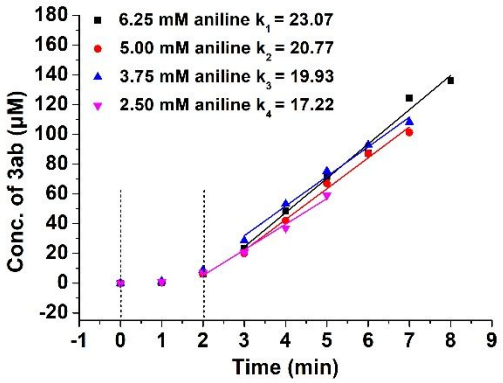

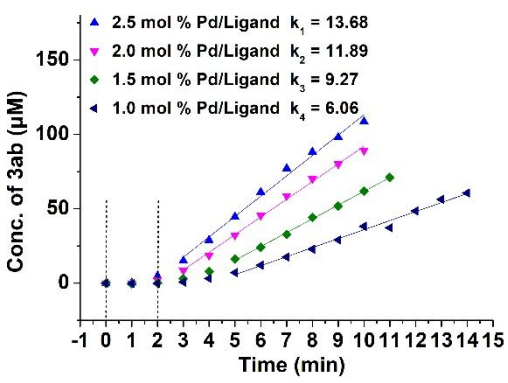

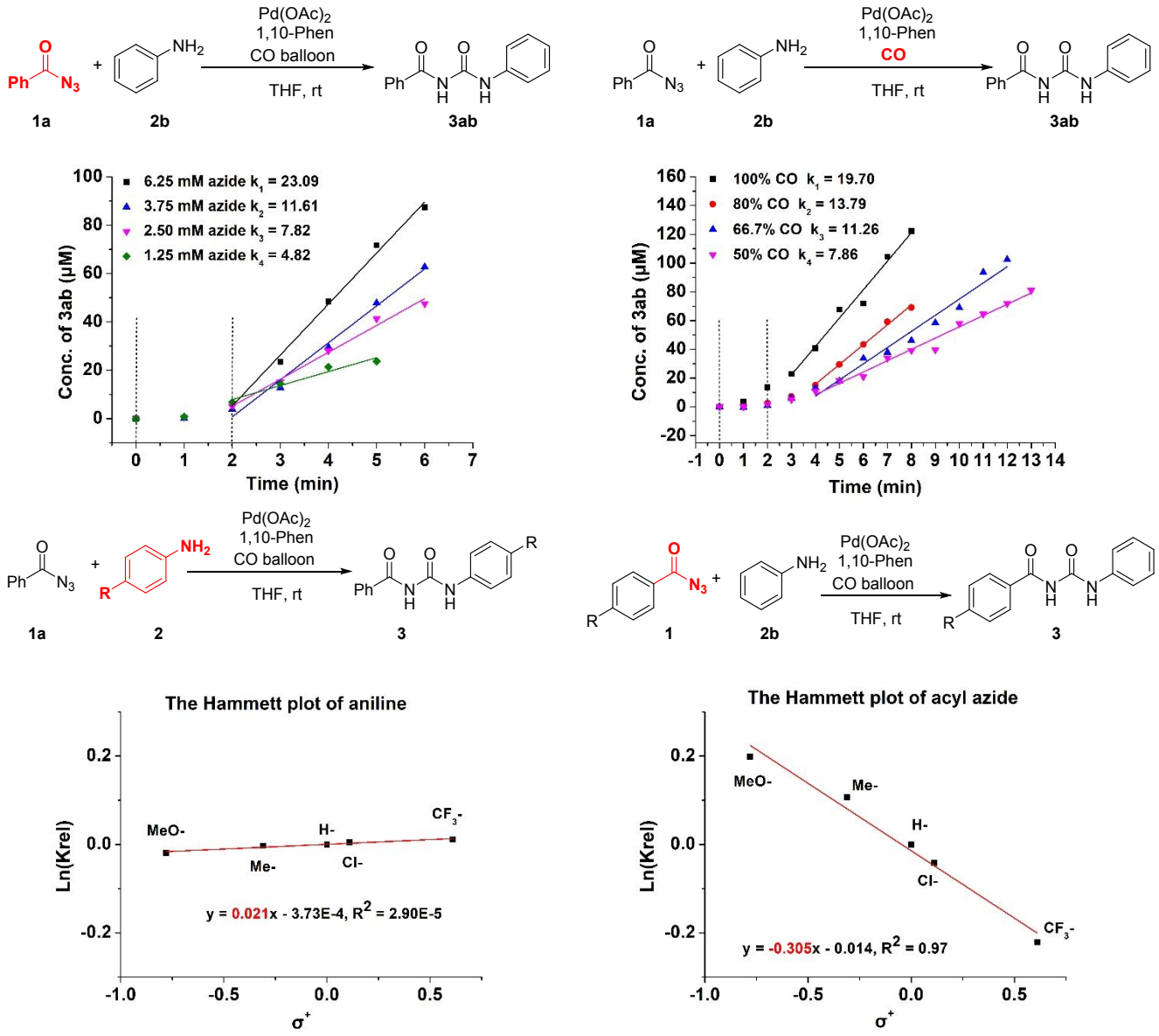

Figure 1. The initial rate kinetic data: a). The rate of different concentration of aniline; b). The rate of different concentration of Pd/1,10-Phen; c). The rate of different concentration of benzoyl azide; d). The rate of different ratio of CO; e). Hammett plot of amine showing the ρ value of ca. +0.021 (R^2 = 0.97); f). Hammett plot of benzoyl azide showing the ρ value of ca. -0.305 (R^2 = 0.97).

Investigation into the Induction Period. The induction period existing in the reactions employing the Pd(II)/ligand catalytic system led us to consider the possibility of precatalyst to catalyst transformation during this period. To further investigate the actual catalytically active Pd species in the catalytic cycle, different palladium catalysts, $Pd(OAc)_2$ for Pd(II) and $Pd_2(dba)_3$ for Pd(0), were tested in the model reaction, and the respective kinetic profiles in a 10 min period were acquired (Figure 2). Again, induction period was observed with 3 mol % $Pd(OAc)_2$/1,10-phen. When 1.5 mol % $Pd_2(dba)_3$/1,10-phen was used instead, the induction period disappeared and higher initial rates were observed (*for more details about*

different Pd catalysts, please see Part 2.7 of the Supporting Information). Based on these results, a likely reason is that during the induction period of the Pd(II)-promoted reaction, a Pd(II) to Pd(0) transformation occurred and Pd(0) species might act as the actual catalyst for the carbonylation reaction.

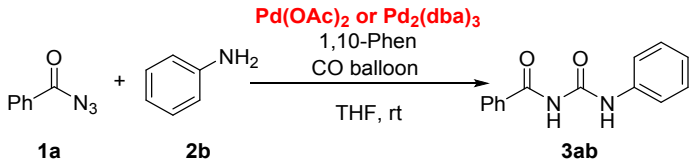

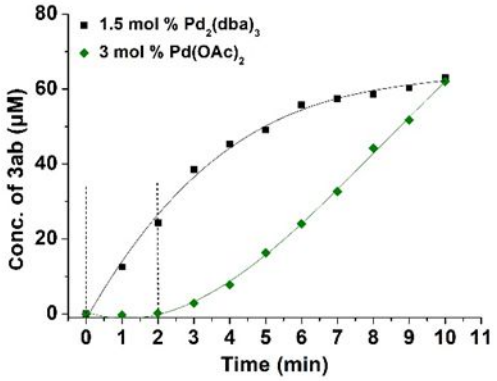

Figure 2. Reaction profile of Pd-catalyzed carbonylation.

Probing the Pd(II) to Pd(0) Transformation by XPS Measurements. Since the valence of palladium has a marked impact on the activity of Pd-catalyzed reactions,[4] it is important to verify the valance of Pd in our catalytic system for acyl azide carbonylation. XPS (X-ray photoelectron spectroscopy) measurements were performed with both the catalyst alone and the reaction mixtures (Figure 3).

We found that Pd(II) species ($Pd(OAc)_2$ and $PdCl_2$) showed peaks at 338 and 343 eV, Pd(0) species ($Pd_2(dba)_3$) showed peaks at 336 and 341 eV. In the normal reaction catalyzed by $Pd(OAc)_2$/1,10-phen under CO, both Pd(II) and Pd(0) peaks could be detected (Figure 3a). However, when CO is absent, only Pd(II) peaks could be detected, and no urea product could be observed (Figure 3b). Moreover, when employing the $PdCl_2$/1,10-phen/NH_4OAc combination as the catalyst, the reaction proceeded well (Table 1, entry 5) and Pd(0) signals were again observed in XPS of the reaction mixture (Figure 3c). In contrast, without acetate anion, $PdCl_2$/1,10-phen could not catalyze the carbonylation, and only Pd(II) signals were found (Figure 3d). These results showed that Pd(0) species was closely related to a "successful" reaction, and thus implied that Pd(0) species, rather than Pd(II) species, acted as the actual catalyst. The Pd(II) to Pd(0) reduction required the presence of both CO and acetate anion, and it was most possible that this reduction process took place during the induction period of the reaction promoted by $Pd(OAc)_2$/1,10-phen.[11]

Based on the above-mentioned results, we proposed that CO was the key reductant to reduce Pd(II) to Pd(0). To confirm this hypothesis and to investigate the oxidative product of CO, we detected the gaseous phase of the reaction mixture employing stoichiometric amount of $Pd(OAc)_2$ by GC-MS. It was found that CO was the only gaseous component at the beginning, while CO_2 was found when the reaction completed (*for more details, please see Part 4 of the Supporting Information*). The formation of CO_2 from CO supported the hypothesis.

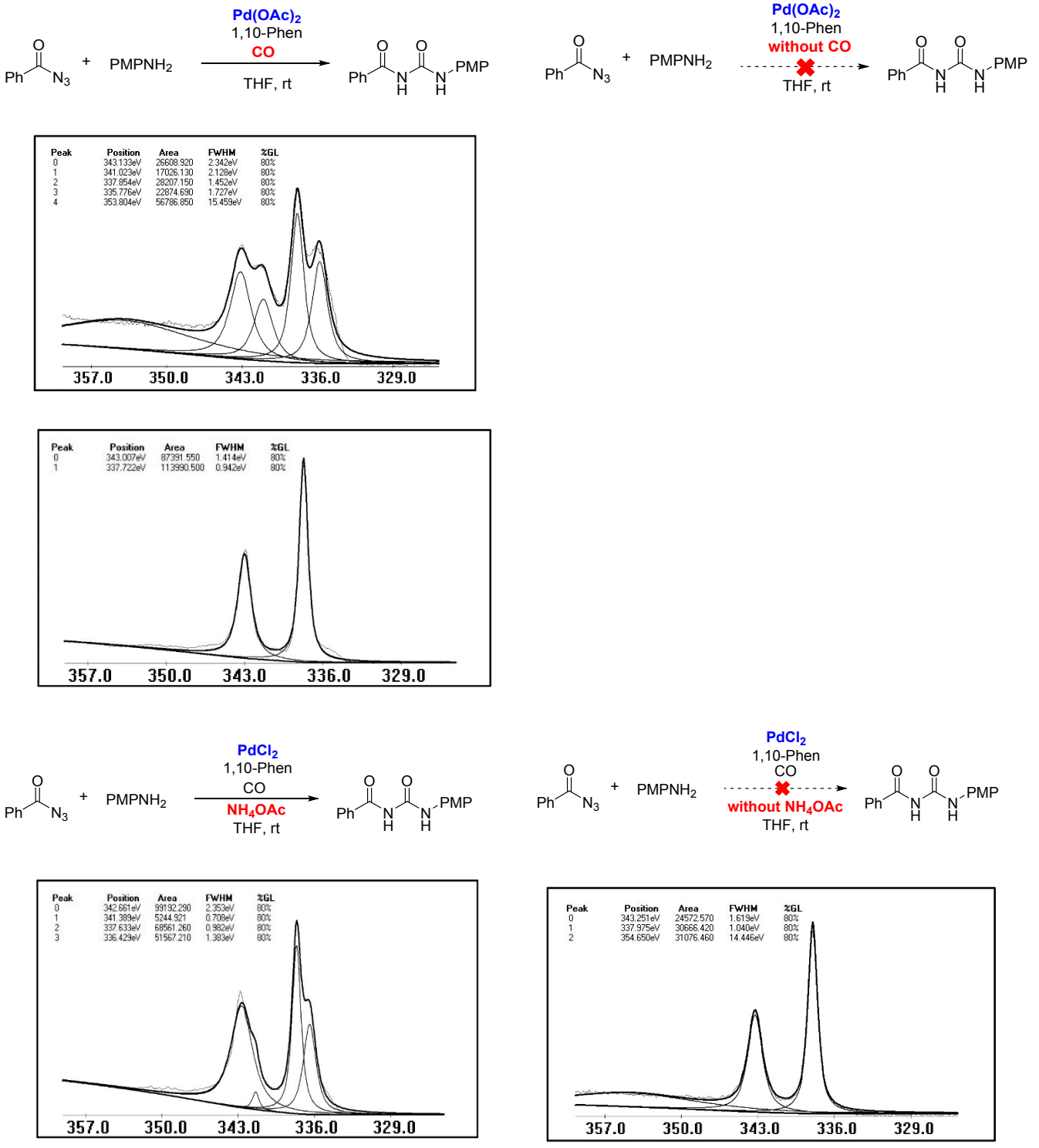

Figure 3. The XPS results of Pd-catalyzed carbonylation: a) $Pd(OAc)_2$ + 1, 10-Phen. + CO + $PhCON_3$ + $PMPNH_2$ (343, 341, 338, 336 eV, 93% yield); b) $Pd(OAc)_2$ + 1, 10-Phen. + $PhCON_3$ + $PMPNH_2$ (343, 338 eV); c) $PdCl_2$ + 1, 10-Phen. + CO + $PhCON_3$ + $PMPNH_2$ + NH_4OAc (343, 341, 338, 336 eV, 92% yield); d) $PdCl_2$ + 1, 10-Phen. + CO + $PhCON_3$ + $PMPNH_2$ (343, 338 eV, no reaction).

To further investigate the role of CO in the reaction, acyl azide (**1a**) was treated with stoichiometric amount of $Pd_2(dba)_3$/1,10-Phen (Scheme 4). Under identical reaction conditions but in the absence of CO, more than 95% of **1a** was recovered after 24 h, which indicated that CO not only acted as a key reagent for Pd(II) to Pd(0) reduction, but also played a vital role in the N_2 releasing step. In other words, the activation of acyl azide would not occur without the participation of CO.

Scheme 4. The Impact of CO.

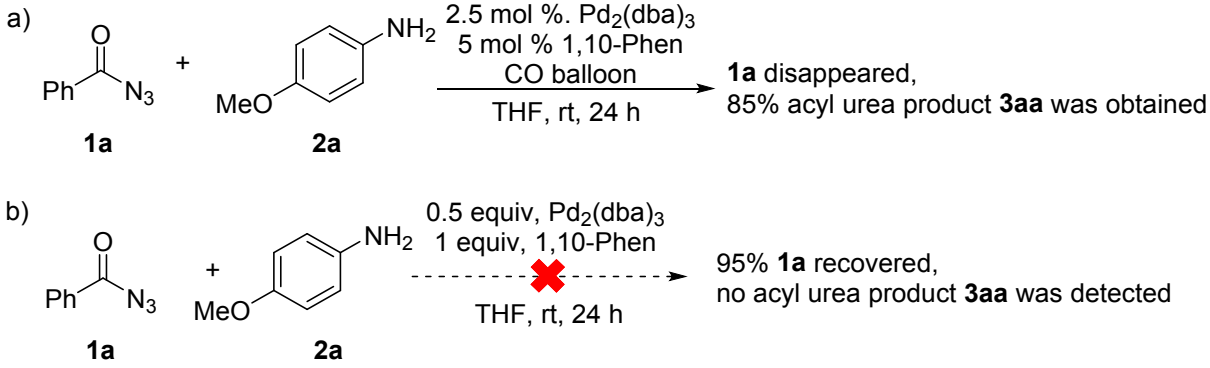

Structure of the Key Pd Species. After confirming the valence of palladium and impact of CO in our reactions, we further studied the structure of the key palladium species in the reaction. The transition-metal-catalyzed carbonylation reactions were important transformations of azides, which were usually catalyzed by Fe, Ni, Co, Cu, Rh, etc. In these transformations, monometallic[12] and bimetallic nitrene[13] complexes were two common types of key intermediates. Another type of key organometallic species was the five-membered metallacycle, which was reported in the stoichiometric reactions of Mn(I), Mo(I) and Os(0) complexes (Figure 4).[14] However, the key Pd-containing complex in Pd-catalyzed carbonylation reaction of azide remains unclear.

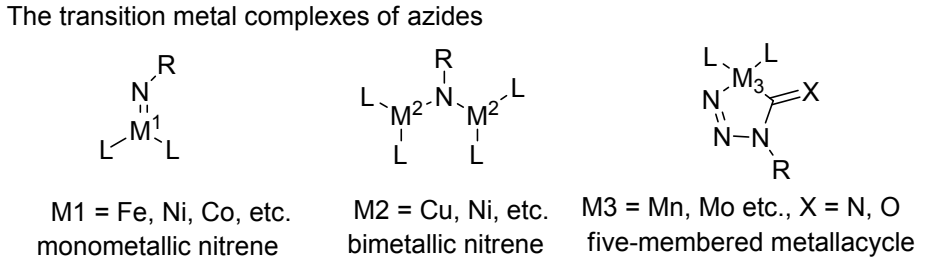

Figure 4. Three intermediates of transition-metal-catalyzed carbonylation of azide

In previous works, Pd-nitrene was proposed to be an important intermediate in carbonylation reaction of azides,[5b-5d] and a bimetallic Pd-nitrene complex ([$Pd_2Cl_2(dppm)_2(\mu$-NR)]) has also been reported to generate through the reaction between $Pd_2Cl_2(dppm)_2$ and azide.[15] In order to distinguish whether or not the bimetallic Pd-nitrene complex was the key species in the catalytic cycle, we performed the following control experiments (Scheme 5). We found that, the combination of 2.5 mol % $Pd_2Cl_2(dppm)_2$, 5 mol % 1,10-Phen, and 20 mol % NH_4OAc, could successfully catalyze the carbonylation reaction of acyl azide **1a**. In contrast, the bimetallic Pd-nitrene complex, $Pd_2Cl_2(dppm)_2(\mu$-NBz), prepared by the reaction of **1a** with $Pd_2Cl_2(dppm)_2$, exhibited no catalytic activity. Even when NH_4OAc was added. Therefore, we believe that the bimetallic Pd(II)-nitrene-type complex is not a key intermediate in Pd-catalyzed carbonylation of acyl azide reactions.

Scheme 5. Bimetallic Pd-nitrene experiments.

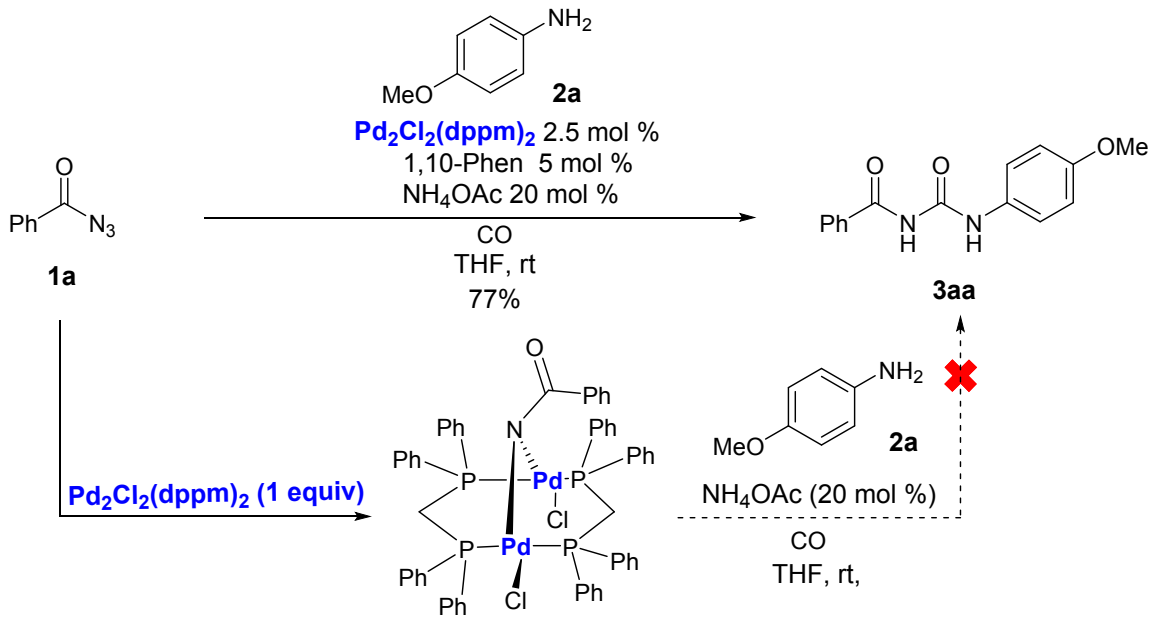

Proposed Catalytic Cycle. Based on the results from the above experimental studies, we could draw a simplified mechanistic picture of the palladium-catalyzed carbonylation of acyl azides (Scheme 6). First the precatalyst, $Pd(OAc)_2$, is reduced by CO in the presence of 1,10-phen ligand to produce the catalytically active Pd(0) species **Int-A**. Coordination of the acyl azide substrate to **Int-A** affords substrate-catalyst complex **Int-B**. Based on the fact that CO is essential for azide activation, we propose that **Int-B** is transformed to a Pd-nitrene complex **Int-C1** or a palladacycle complex **Int-C2**. Subsequent carbonylation (insertion of CO) leads to the Pd-isocyanate complex **Int-D**. Ligand exchange by excess CO releases the isocyanate product and regenerates the catalyst **Int-A**. Finally, nucleophilic attack of an amine to the isocyanate affords the acyl urea product.

Scheme 6. Proposed Catalytic Cycle.

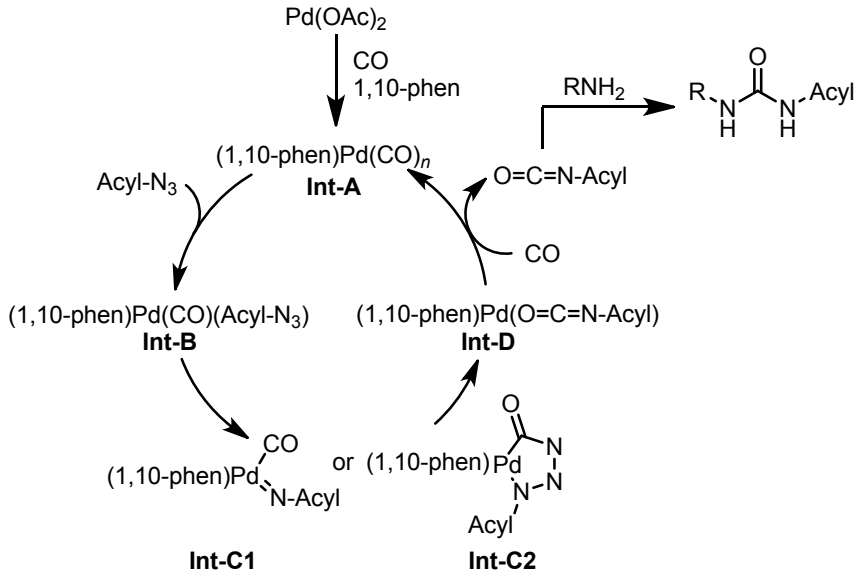

DFT Computational Study. To gain a deeper understanding of the carbonylation mechanism, DFT calculations were carried out using the Gaussian 09 program package (*for more details, see Part 5 of the Supporting Information*).[16] The carbonylation of acetyl azide to afford acetyl isocyanate was used as the model reaction in the calculation. We studied the potential energy surfaces of both Pd(II)- and Pd(0)-catalyzed scenarios to further confirm the accurate catalytic species.

At the beginning, various Pd(II)-catalyzed carbonylation pathways *via* either monometallic or bimetallic nitrene intermediates were calculated. However, the activation barriers, in terms of Gibbs free energy, of these pathways were too high to be reasonable (*see Part 5.1 of the Supporting Information*). These results excluded the possibility of Pd(II)-species acting as active catalysts for acyl azide carbonylation, which is in agreement with the conclusions drawn from the experimental study.

Therefore, we set out to calculate the Pd(0)-initiated pathway. First, the reduction process of Pd(II) was calculated (*see Part 5.2 of the Supporting Information*) to proceed with an activation barrier of 21.4 kcal/mol, which is reasonable for a rapid transformation.[11] Subsequently, the Pd(0)/1,10-phen intermediates with two CO ligands (complex **5**), formed through the coordination of 1,10-phen to *in situ* generated $Pd^0(CO)_2$, was calculated. It was found that complex **5** adopted Pd(0) configuration, in which the C-Pd-C angle is 120.9° and two Pd-C bonds are 1.85 Å in length. Dissociation of CO from intermediate **5** generates a coordinatively unsaturated complex **6**, in which the bond length between the Pd center and CO is 1.85 Å, and 1,10-phen, Pd, and CO formed an approximate plane to provide an open space for azide coordination. It is notable that complex **5** is thermodynamically more favorable than complex **6** in terms of Gibbs free energy under standard conditions.

Coordination of acyl azide to the Pd center produced two different structures: **7a** with the coordination of the terminal nitrogen, and **7b** with the coordination of the α-nitrogen, with **7b** thermodynamically more favorable. Following the normal N_2 release mechanism of organic azides, we located transition state **TS-1c** that corresponds to direct N_2 elimination from complex **7b**. The activation barrier of this step is 22 kcal/mol (from **7b** to **TS-1c**), and an overall barrier is 31.5 kcal/mol (from **5** to **TS-1c**). Meanwhile, two other azide activation transition states leading to five-membered palladacycles *via* oxidative cyclization, **TS-1a** and **TS-1b**, were also located. **TS-1a** represents the C-N bond forming process between the CO and α-nitrogen of the end-on coordinated azide, with an activation barrier of 9.9 kcal/mol; while **TS-1b**

relates to the C-N bond forming process between the CO and the terminal nitrogen of the side-on coordinated azide, with an activation barrier of 13.5 kcal/mol. In terms of overall activation barrier, **TS-1a** is more favorable than **TS-1b** (by 2.1 kcal/mol), and **TS-1c** is much less favored.

The oxidative cyclization transition states lead to exergonic formation of two five-membered palladacycle species **8a** and **8b**, with complex **8b** being slightly more stable than **8a** by 0.9 kcal/mol. In complex **8a**, the length of N(azide)-C(CO) bond is 1.46 Å, suggesting a C-N single bond character. The Pd-C(CO) bond and Pd-N(azide) bond lengths are 1.98 and 2.00 Å, respectively. Complex **8a** subsequently releases N_2 with a very low barrier (1.7 kcal/mol)[17] *via* **TS-2a** to give a Pd(0) species **10** exergonically (ΔG = −56.2 kcal/mol), in which Pd-N, Pd-C and C-N bonds are 2.09, 1.99 and 1.30 Å in length, respectively. In the last step, reductive elimination of complex **10** together with ligand exchange with CO generates the free acetyl isocyanate and complex **6** in a thermodynamically favorable manner (ΔG = -17.2 kcal/mol). On the other hand, the reaction path of intermediate **8b** was also examined. A transition state **TS-2b** corresponds to N_2 elimination from complex **8b** was located, which leads to Pd-nitrene intermediate **9**. Although nitrene complex **9** has the potential to undergo CO insertion to form the desired product complex **10**, this reaction pathway is thermodynamically less favorable due to the high activation barrier of the N_2 releasing step (**TS-2b**).

Review the complete potential energy surface (Figure 5), the overall activation barrier for the preferred reaction pathway (**5 → 6 → 7a → TS-1a → 8a → TS-2a → 10**) is 20.9 kcal/mol in terms of Gibbs free energy. The formation of five-membered palladacycle through oxidative cyclization (**TS-1a**) is the turnover-limiting step. The computational results are in agreement with our kinetic study, since a rate-limiting oxidative cyclization step should be first order on both Pd and acyl azide. The fact that dicarbonyl complex **5** is more stable than monocarbonyl complex **6** suggested possible inhibition of the reaction under high [CO]. While in a low [CO] regime, positive dependence on [CO] is expected because CO is an essential substrate for the reaction (*for more details about the free energy corrections under different CO pressures, see Part 5.3 of the Supporting Information*). Indeed, both the positive dependence of the initial rate on CO pressure and the inhibition of the reaction under high CO pressure was observed, which was in good agreement with the DFT results. The calculation also supported the conclusion drawn from the experimental study that Pd(0) species, rather than Pd(II) species, initiates the azide activation process. However, in this reaction system the commonly accepted nitrene mechanism is not operable.

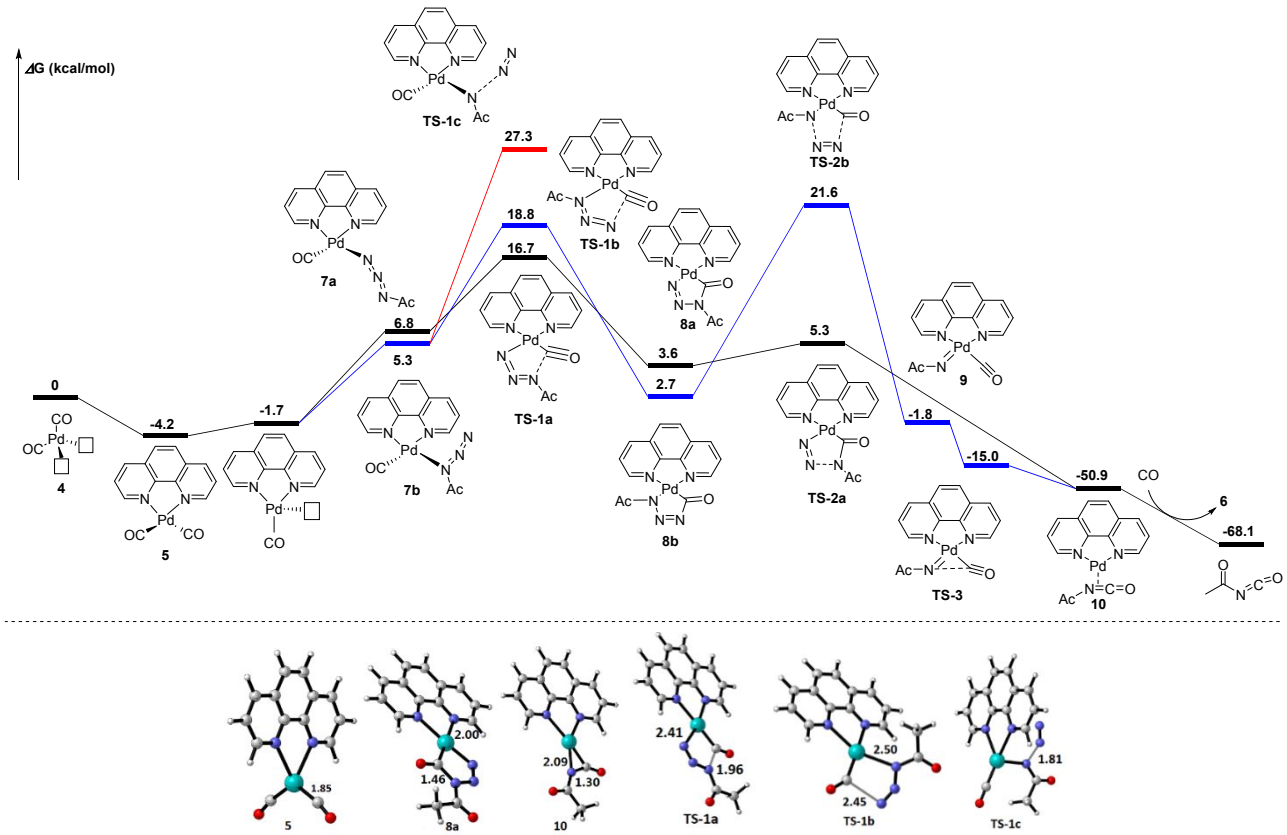

Figure 5. Energy profile of the overall catalytic cycle and 3D structure of selected computed transition states

Conclusions

In summary, we have developed a Pd-catalyzed carbonylation of acyl azides and presented a detailed mechanistic study. The carbonylation reaction of acyl azides with excellent substrate scope provides facile access to acyl ureas in mild conditions. Control experiments disclosed that the reaction is initiated by Pd(0) species rather than Pd(II) species. Kinetic studies and DFT calculations showed that the isocyanate generation step is the turnover-limiting step, N_2 releasing and CO insertion occur at the same time, and a five-membered palladacycle complex is a key intermediate. Furthermore, this Pd-catalyzed carbonylation represents a new mechanistic model for Pd-catalyzed reaction of azide with N_2 releasing process. We anticipate more Pd-catalyzed reactions of azides could be realized under this mode.

Experimental section

Caution All these azide compounds mentioned above are potentially explosive substances. Mechanical actions involving scratching or scraping must be avoided. In addition, all of the compounds must be synthesized on a small scale. Manipulations must be carried out in a hood behind a safety shield. Eye protection and latex gloves must be worn at all times.

General Information. All reactions were performed in a Schlenk reaction flask. All solvents were purchased from Sinopharm Chemical Reagent, and THF was redistilled by sodium. The boiling point of

petroleum ether is between 60 and 90 °C. For chromatography, 200-300 mesh silica gel (Qingdao, China) was employed. ^{1}H and ^{13}C NMR spectra were recorded at 400 MHz and 100 MHz with Varian Mercury 400 spectrometer at ambient temperature. Chemical shifts are reported in ppm relative to chloroform (^{1}H, δ 7.26; ^{13}C, δ 77.00), DMSO (^{1}H, δ 2.50; ^{13}C, δ 39.52). IR spectra were recorded with a Nicolet AVATAR 330 FT-IR spectrometer. Mass spectra were obtained on a Waters Auto Purification LC/MS system. HMRS were obtained on a Bruker Apex IV FTMS spectrometer. All palladium catalysts were purchased from Sigma-Aldrich. All ligands were purchased from Energy Chemical. All Acyl chlorides and amines are commercially available.

Typical process for synthesis of acyl azide.[18] In 50 mL flask, benzoyl chloride (1406 mg, 1.161 mL, 10 mmol) solute into 15 mL of acetone, and sodium azide (780 mg, 12 mmol) was added slowly at 0 °C. The mixture was stirred until benzoyl chloride cannot observed at TLC. And then filter for removing sodium azide and sodium chloride, and removing acetone under reduced pressure. Finally, the residue was purified at flash chromatography with petroleum and ethyl acetate as eluent (PE: EA = 30: 1) and obtained benzoyl azide **1a** (1351 mg, 92%).

*N-((4-methoxyphenyl)carbamoyl)benzamide (**3aa**)*[19]: In a Schlenk reaction flask, benzoyl azide **1a** (29 mg, 0.20 mmol), Pd(OAc)2 (2 mg, 0.01 mmol), 1, 10-phenatheroline (2 mg, 0.01 mmol), 4-methoxyaniline **2a** (30 mg, 0.24 mmol), and THF (3 ml) were added, the flask was sealed and evacuated to a vacuum of 15 mmHg and fitted with a CO balloon. The mixture was stirred at room temperature until 1a disappeared as judged by TLC. The solution was removed under reduced pressure. The residue was then diluted with 20 ml DCM, washed with 20 ml 1M HCl, and the aqueous layer was extracted with DCM (3×20 ml). All organic extracts were pooled, dried over $MgSO_4$, and concentrated under reduced pressure to leave a residue which was purified by silica gel chromatography with DCM and ethyl ethoxyethane as eluent (DCM: Et_2O = 15:1) to afford product **3aa** (52 mg, 98%). White solid, m. p. = 210-211 °C, ^{1}H NMR (400 MHz, DMSO-d6) δ 10.96 (s, 1H), 10.67 (s, 1H), 8.06 – 7.96 (m, 2H), 7.69 – 7.62 (m, 1H), 7.59 – 7.45 (m, 4H), 6.98 – 6.85 (m, 2H), 3.75 (s, 3H) ppm. $^{13}C\{^{1}H\}$ NMR (100 MHz, DMSO-d6) δ 168.6, 155.7, 151.1, 132.9, 132.3, 130.5, 128.5, 128.2, 121.6, 114.1, 55.2 ppm.

*N-(phenylcarbamoyl)benzamide (**3ab**)*[20]: white solid, 45 mg, 94%, m. p. = 194-195 °C, ^{1}H NMR (400 MHz, DMSO-d6) δ 11.02 (s,1H), 10.83 (s, 1H), 8.08 – 7.94 (m, 2H), 7.66 (ddd, *J = 6.8, 4.0, 1.3* Hz, 1H), 7.59 (dt, *J = 8.8*, 1.7 Hz, 2H), 7.57 – 7.52 (m, 2H), 7.40 – 7.33 (m, 2H), 7.16 – 7.08 (m, 1H) ppm. $^{13}C\{^{1}H\}$ NMR (100 MHz, DMSO-d6) δ 168.6, 151.1, 137.6, 133.0, 132.2, 128.9, 128.5, 128.2, 123.7, 119.8 ppm.

*N-((4-(trifluoromethyl)phenyl)carbamoyl)benzamide (**3ac**)*: white solid, 56 mg, 90%, m. p. = 220-221 °C, ^{1}H NMR (400 MHz, DMSO-d6) δ 11.15 (s, 1H), 11.06 (s, 1H), 8.03 (dt, *J = 8.5, 1.7* Hz, 2H), 7.83 (d, *J = 8.5* Hz, 2H), 7.72 (d, *J = 8.6* Hz, 2H), 7.69 – 7.64 (m, 1H), 7.58 – 7.52 (m, 2H) ppm. $^{13}C\{^{1}H\}$ NMR (100 MHz, DMSO-d6) δ 168.7, 151.2, 141.4, 133.2, 132.1, 128.6, 128.3, 126.2 (q, *J* = 7.9 Hz), 124.4 (q, *J* = 278.4 Hz), 123.6, 119.8 ppm. IR (neat) 1707, 1607, 1563, 1333, 1282, 1112, 1072, 710 cm^{-1}. HRMS (ESI^{+}) m/z: [M + H] calcd for $C_{15}H_{12}F_3N_2O_2$: 309.0845, found: 309.0849.

*N-(p-tolylcarbamoyl)benzamide (**3ad**)*[19]: white solid, 42 mg, 82%, m. p. = 220-221 °C, ^{1}H NMR (400 MHz, DMSO-d6) δ 11.01 (s, 1H), 10.77 (s, 1H), 8.08 – 7.96 (m, 2H), 7.69 – 7.61 (m, 1H), 7.58 – 7.50 (m, 2H), 7.49 – 7.42 (m, 2H), 7.25 – 7.06 (m, 2H), 2.27 (s, 3H) ppm. $^{13}C\{^{1}H\}$ NMR (100 MHz, DMSO-d6) δ 168.7, 151.1, 135.1, 133.0, 132.8, 132.3, 129.4, 128.6, 128.3, 119.8, 20.4 ppm.

*N-(m-tolylcarbamoyl)benzamide (**3ae**)*: white solid, 48 mg, 94%, m. p. = 160-162 °C, ^{1}H NMR (400 MHz, DMSO-d6) δ 11.03 (s, 1H), 10.81 (s, 1H), 8.07 – 7.99 (m, 2H), 7.71 – 7.64 (m, 1H), 7.54 (dd, *J = 10.6,*

4.8 Hz, 2H), 7.39 (d, *J = 6.5* Hz, 2H), 7.26 – 7.20 (m, 1H), 6.93 (d, *J = 7.7* Hz, 1H), 2.31 (s, 3H) ppm. $^{13}C\{^1H\}$ NMR (100 MHz, DMSO-d6) δ 168.8, 151.1, 138.4, 137.5, 133.1, 132.3, 128.9, 128.6, 128.3, 124.5, 120.3, 116.9, 21.2 ppm. IR (neat) 1703, 1673, 1598, 1566, 1506, 1275, 1288, 780 cm^{-1}. HRMS (ESI^+) m/z: [M + H] calcd for $C_{15}H_{15}N_2O_2$: 255.1128, found: 255.1131.

*N-(o-tolylcarbamoyl)benzamide (**3af**)*[19]: white solid, 51 mg, >98%, m. p. = 206-218 °C, ^1H NMR (400 MHz, DMSO-d6) δ 11.12 (s, 1H), 10.86 (s, 1H), 8.10 – 7.98 (m, 3H), 7.66 (ddd, *J = 6.8, 4.0, 1.2* Hz, 1H), 7.54 (dd, *J = 10.6, 4.8* Hz, 2H), 7.28 – 7.20 (m, 2H), 7.09 – 7.02 (m, 1H), 2.32 (s, 3H) ppm. $^{13}C\{^1H\}$ NMR (100 MHz, DMSO-d6) δ 169.1, 151.2, 136.1, 133.1, 132.2, 130.3, 128.6, 128.4, 127.6, 126.5, 123.9, 120.9, 17.7 ppm.

*N-((4-fluorophenyl)carbamoyl)benzamide (**3ag**)*[20]: white solid, 45 mg, 88%, m. p. = 200-202 °C, ^1H NMR (400 MHz, DMSO-d6) δ 11.06 (s, 1H), 10.81 (s, 1H), 8.08 – 7.94 (m, 2H), 7.73 – 7.58 (m, 3H), 7.58 – 7.48 (m, 2H), 7.26 – 7.11 (m, 2H) ppm. $^{13}C\{^1H\}$ NMR (100 MHz, DMSO-d6) δ 168.6, 158.4 (d, *J = 240.4* Hz), 151.3, 133.9 (d, *J = 2.6* Hz), 133.0, 132.3, 128.5, 128.3, 121.9 (d, *J = 6.6* Hz), 115.5 (d, *J = 29.6* Hz) ppm.

*N-((4-chlorophenyl)carbamoyl)benzamide (**3ah**)*[21]: white solid, 53 mg, 96%, m. p. = 232-233 °C, ^1H NMR (400 MHz, DMSO-d6) δ 11.09 (s, 1H), 10.87 (s, 1H), 8.07 – 7.96 (m, 2H), 7.70 – 7.60 (m, 3H), 7.59 – 7.49 (m, 2H), 7.41 (d, *J = 8.8 Hz*, 2H) ppm. $^{13}C\{^1H\}$ NMR (100 MHz, DMSO-d6) δ 168.7, 151.2, 136.7, 133.1, 132.2, 128.9, 128.6, 128.3, 127.4, 121.5 ppm.

*N-((4-bromophenyl)carbamoyl)benzamide (**3ai**)*[19]: white solid, 59 mg, 92%, m. p. = 233-234 °C, ^1H NMR (400 MHz, DMSO-d6) δ 11.10 (s, 1H), 10.87 (s, 1H), 8.09 – 7.95 (m, 2H), 7.71 – 7.40 (m, 7H) ppm. $^{13}C\{^1H\}$ NMR (100 MHz, DMSO-d6) δ 168.7, 151.1, 137.1, 133.1, 132.2, 131.8, 128.6, 128.3, 121.9, 115.4 ppm.

*N-((4-iodophenyl)carbamoyl)benzamide (**3aj**)*: white solid, 68 mg, 93%, m. p. = 236-238 °C, ^1H NMR (400 MHz, DMSO-d6) δ 11.09 (s, 1H), 10.86 (s, 1H), 8.06 – 7.97 (m, 2H), 7.73 – 7.61 (m, 3H), 7.59 – 7.49 (m, 2H), 7.49 – 7.40 (m, 2H) ppm. $^{13}C\{^1H\}$ NMR (100 MHz, DMSO-d6) δ 169.1, 165.8, 151.5, 138.0, 133.6, 132.7, 129.1, 128.8, 122.6, 87.8 ppm. IR (neat) 1698, 1664, 1589, 1548, 1507, 1482, 1271, 1226 cm^{-1}. HRMS (ESI^+) m/z: [M + Na] calcd $C_{14}H_{11}IN_2O_2Na$ for: 388.9757, found: 388.9764.

*N-((2-chlorophenyl)carbamoyl)benzamide (**3ak**)*[22]: white solid, 52 mg, 95%, m. p. = 220-221 °C, ^1H NMR (400 MHz, DMSO-d6) δ 11.45 (s, 1H), 11.27 (s, 1H), 8.33 (dd, *J = 8.3, 1.5* Hz, 1H), 8.10 – 7.97 (m, 2H), 7.69 – 7.64 (m, 1H), 7.58 – 7.51 (m, 2H), 7.41 – 7.36 (m, 1H), 7.15 (ddd, *J = 8.0, 7.5, 1.6* Hz, 1H) ppm. $^{13}C\{^1H\}$ NMR (100 MHz, DMSO-d6) δ 169.1, 151.1, 134.7, 133.2, 132.0, 129.4, 128.6, 128.4, 127.9, 124.7, 122.4, 121.5 ppm.

*N-((4-cyanophenyl)carbamoyl)benzamide (**3al**)*: white solid, 52 mg, >98%, m. p. = 262-263 °C, ^1H NMR (400 MHz, DMSO-d6) δ 11.18 (s, 1H), 11.07 (s, 1H), 8.03 (d, *J = 7.6* Hz, 2H), 7.82 (s, 4H), 7.66 (d, *J = 7.4* Hz, 1H), 7.61 – 7.51 (m, 2H) ppm. $^{13}C\{^1H\}$ NMR (100 MHz, DMSO-d6) δ 169.1, 151.6, 142.6, 133.9, 133.7, 132.6, 129.1, 128.8, 120.4, 119.4, 105.9 ppm. IR (Neat) 1720, 1596, 1549, 1481, 1412, 1281, 1235, 759 cm^{-1}. HRMS (ESI^+) m/z: [M + H] calcd $C_{15}H_{12}N_3O_2$ for: 266.0923, found: 266.0922.

*N-([1,1'-biphenyl]-4-ylcarbamoyl)benzamide (**3am**)* [20]: white solid, 47 mg, 75%, m. p. = 223-235 °C, ^1H NMR (400 MHz, DMSO-d6) δ 11.09 (s, 1H), 10.92 (s, 1H), 8.10 – 7.98 (m, 2H), 7.74 – 7.61 (m, 7H), 7.60 – 7.51 (m, 2H), 7.50 – 7.42 (m, 2H), 7.38 – 7.30 (m, 1H) ppm. $^{13}C\{^1H\}$ NMR (100 MHz, DMSO-d6) δ 169.2, 152.1, 151.6, 140.1, 137.6, 136.0, 132.8, 129.5, 129.1, 128.8, 127.7, 126.8, 120.8 ppm.

*methyl 4-(3-benzoylureido)benzoate (**3an**)*: white solid, 54 mg, 90%, m. p. = 226-228 °C, ^{1}H NMR (400 MHz, DMSO-d6) δ 11.15 (s, 1H), 11.08 (s, 1H), 8.03 (d, *J = 7.3* Hz, 2H), 7.96 (d, *J = 8.7* Hz, 2H), 7.74 (d, *J = 8.7* Hz, 2H), 7.70 – 7.60 (m, 1H), 7.58 – 7.50 (m, 2H), 3.83 (s, 3H) ppm. ^{13}C{^{1}H} NMR (100 MHz, DMSO-d6) δ 168.7, 165.7, 151.0, 142.2, 133.2, 132.2, 130.4, 128.6, 128.3, 124.4, 119.1, 104.5, 51.9 ppm. IR (Neat) 1664, 1606, 1577, 1464, 1448, 1281, 1173, 838 cm^{-1}. HRMS (ESI$^+$) m/z: [M + H] calcd $C_{16}H_{15}N_2O_4$ for: 299.1032, found: 299.1024.

*N-((4-(4,4,5,5-tetramethyl-1,3,2-dioxaborolan-2-yl)phenyl)carbamoyl)benzamide (**3ao**)*: white solid, 55 mg, 75%, m. p. = 222-224 °C, ^{1}H NMR (400 MHz, DMSO-d6) δ 11.11 (s, 1H), 10.98 (s, 1H), 8.02 (d, J = 7.5 Hz, 2H), 7.70 – 7.58 (m, 5H), 7.54 (t, *J = 7.6* Hz, 2H), 1.29 (s, 12H) ppm. ^{13}C{^{1}H} NMR (100 MHz, DMSO-d6) δ 169.3, 151.5, 141.0, 136.0, 133.6, 132.7, 129.1, 128.8, 119.2, 84.0, 25.2 ppm. IR (Neat) 1702, 1674, 1592, 1543, 1474, 1360, 1269, 1144 cm^{-1}. HRMS (ESI$^+$) m/z: [M + H] calcd $C_{20}H_{24}BN_2O_4$ for: 367.1827, found: 367.1829.(without reference, without spectrum)

*N-(naphthalen-1-ylcarbamoyl)benzamide (**3ap**)*[19]: white solid, 37 mg, 64%, m. p. = 211-213 °C, ^{1}H NMR (400 MHz, DMSO-d6) δ 11.54 (s, 1H), 11.29 (s, 1H), 8.20 – 8.13 (m, 1H), 8.14 – 8.09 (m, 2H), 8.09 – 8.04 (m, 1H), 8.03 – 7.95 (m, 1H), 7.81 – 7.72 (m, 1H), 7.73 – 7.65 (m, 2H), 7.64 – 7.51 (m, 3H) ppm. ^{13}C{^{1}H} NMR (100 MHz, DMSO-d6) δ 169.4, 151.6, 133.6, 133.2, 132.7, 132.3, 132.2, 128.7, 128.6, 128.5, 126.7, 125.9, 125.6, 124.4, 120.4, 118.1 ppm.

*N-(benzylcarbamoyl)benzamide (**3aq**)*[23]: white solid, 41 mg, 80%, m. p. = 142-143 °C, ^{1}H NMR (400 MHz, DMSO-d6) δ 10.77 (s, 1H), 9.08 (t, *J = 5.9* Hz, 1H), 8.00 – 7.87 (m, 2H), 7.66 – 7.58 (m, 1H), 7.55 – 7.47 (m, 2H), 7.37 – 7.23 (m, 5H), 4.46 (d, *J = 6.0* Hz, 2H) ppm. ^{13}C{^{1}H} NMR (100 MHz, DMSO-d6) δ 168.3, 153.6, 139.2, 132.8, 132.5, 128.5, 128.4, 128.1, 127.2, 126.9, 42.7 ppm.

*N-(butylcarbamoyl)benzamide (**3ar**)*[24]: white solid, 22 mg, 50%, m. p. = 69-70 °C, ^{1}H NMR (400 MHz, DMSO-d6) δ 10.67 (s, 1H), 8.67 (t, *J = 5.6* Hz, 1H), 8.00 – 7.93 (m, 2H), 7.67 – 7.57 (m, 1H), 7.56 – 7.43 (m, 2H), 3.23 (dd, *J = 12.8, 6.9* Hz, 2H), 1.53 – 1.44 (m, 2H), 1.39 – 1.26 (m, 2H), 0.90 (t, *J = 7.3* Hz, 3H) ppm. ^{13}C{^{1}H} NMR (100 MHz, DMSO-d6) δ 168.2, 153.5, 132.7, 132.6, 128.5, 128.1, 38.7, 31.3, 19.6, 13.7 ppm.

*N-(cyclohexylcarbamoyl)benzamide (**3as**)*[25]: white solid, 46 mg, 94%, m. p. = 146-147 °C, ^{1}H NMR (400 MHz, DMSO-d6) δ 10.68 (s, 1H), 8.67 (d, *J = 7.6* Hz, 1H), 8.12 – 7.85 (m, 2H), 7.61 (dd, *J = 10.8, 4.0* Hz, 1H), 7.54 – 7.41 (m, 2H), 3.73 – 3.52 (m, 1H), 1.95 – 1.14 (m, 10H) ppm. ^{13}C{^{1}H} NMR (100 MHz, DMSO-d6) δ 168.4, 152.6, 132.7, 132.6, 128.5, 128.1, 47.8, 32.3, 25.1, 24.2.

*ethyl benzoylcarbamate (**3at**)*[19]: white solid, 25 mg, 65%, m. p. = 89-90 °C, ^{1}H NMR (400 MHz, DMSO-d6) δ 10.93 (s, 1H), 8.11 – 7.73 (m, 2H), 7.67 – 7.57 (m, 1H), 7.54 – 7.33 (m, 2H), 4.18 (q, *J = 7.1* Hz, 2H), 1.26 (t, *J = 7.1* Hz, 3H) ppm. ^{13}C{^{1}H} NMR (100 MHz, DMSO-d6) δ 165.8, 151.6, 133.2, 132.5, 128.3, 128.3, 61.0, 14.2 ppm.

*4-methoxy-N-(phenylcarbamoyl)benzamide (**3bb**)*[20]: white solid, 53 mg, >98%, m. p. = 216-217 °C, ^{1}H NMR (400 MHz, DMSO-d6) δ 10.94 (s, 1H), 10.89 (s, 1H), 8.12 – 7.99 (m, 2H), 7.64 – 7.51 (m, 2H), 7.42 – 7.26 (m, 2H), 7.17 – 6.95 (m, 3H), 3.85 (s, 3H) ppm. ^{13}C{^{1}H} NMR (100 MHz, DMSO-d6) δ 167.9, 163.1, 151.3, 137.7, 130.5, 129.0, 124.1, 123.7, 119.8, 113.9, 55.5 ppm.

*N-(phenylcarbamoyl)-4-(trifluoromethyl)benzamide (**3cb**)*[26]: white solid, 58 mg, 94%, m. p. = 220-221 °C, ^{1}H NMR (400 MHz, DMSO-d6) δ 11.28 (s, 1H), 10.69 (s, 1H), 8.37 – 8.07 (m, 2H), 8.09 – 7.82 (m, 2H), 7.71 – 7.53 (m, 2H), 7.47 – 7.22 (m, 2H), 7.25 – 6.79 (m, 1H) ppm. ^{13}C{^{1}H} NMR (100 MHz, DMSO-

d6) δ 167.7, 150.8, 137.5, 136.3, 132.4 (q, *J = 32.0* Hz), 129.2, 129.0, 125.5 (q, *J = 3.8* Hz), 123.9, 123.7 (q, *J = 272.8* Hz), 119.9 ppm.

*4-methyl-N-(phenylcarbamoyl)benzamide (**3db**)*[26]: white solid, 50 mg, >98%, m. p. = 198-199 °C, ^{1}H NMR (400 MHz, CDCl3) δ 11.02 (s, 1H), 9.84 (s, 1H), 7.97 (d, *J = 8.0* Hz, 2H), 7.61 (d, *J = 8.5* Hz, 2H), 7.39 – 7.33 (m, 2H), 7.31 (d, *J = 8.2 Hz*, 2H), 7.19 – 7.12 (m, 1H). ^{13}C NMR (100 MHz, CDCl3) δ 168.6, 152.2, 144.3, 137.4, 129.6, 129.4, 129.1, 128.2, 124.5, 120.5, 21.8 ppm.

*3-methyl-N-(phenylcarbamoyl)benzamide (**3eb**)*[26]: white solid, 50 mg, 98%, m. p. = 167-168 °C, ^{1}H NMR (400 MHz, DMSO-d6) δ 10.97 (s, 1H), 10.84 (s, 1H), 7.89 – 7.77 (m, 2H), 7.65 – 7.53 (m, 2H), 7.51 – 7.39 (m, 2H), 7.38 – 7.29 (m, 2H), 7.17 – 7.00 (m, 1H), 2.38 (s, 3H) ppm. ^{13}C{^{1}H} NMR (100 MHz, CDCl3) δ 168.8, 151.1, 138.0, 137.6, 132.2, 129.0, 128.8, 128.8, 128.5, 125.5, 123.7, 119.8, 20.8.

*2-methyl-N-(phenylcarbamoyl)benzamide (**3fb**)*[26]: white solid, 36 mg, 71%, m. p. = 167-168 °C, ^{1}H NMR (400 MHz, DMSO-d6) δ 11.01 (s, 1H), 10.67 (s, 1H), 7.61 – 7.56 (m, 2H), 7.54 – 7.48 (m, 2H), 7.47 – 7.40 (m, 1H), 7.39 – 7.24 (m, 4H), 7.16 – 7.06 (m, 1H), 2.41 (s, 3H) ppm. ^{13}C{^{1}H} NMR (100 MHz, DMSO-d6) δ 171.4, 150.8, 137.6, 135.9, 134.4, 130.8, 130.7, 129.0, 127.8, 125.6, 123.7, 119.7, 19.5 ppm.

*4-chloro-N-(phenylcarbamoyl)benzamide (**3gb**)*[27]: white solid, 54 mg, 98%, m. p. = 194-196 °C, ^{1}H NMR (400 MHz, DMSO-d6) δ 11.12 (s, 1H), 10.74 (s, 1H), 8.10 – 7.96 (m, 2H), 7.64 – 7.60 (m, 2H), 7.60 – 7.55 (m, 2H), 7.39 – 7.31 (m, 2H), 7.15 – 7.08 (m, 1H) ppm. ^{13}C{^{1}H} NMR (100 MHz, DMSO-d6) δ 167.7, 150.9, 137.9, 137.5, 131.2, 130.3, 129.0, 128.7, 123.8, 119.9 ppm.

*4-bromo-N-(phenylcarbamoyl)benzamide (**3hb**)*: white solid, 53 mg, 83%, m. p. = 234-235 °C, ^{1}H NMR (400 MHz, DMSO-d6) δ 11.12 (s, 1H), 10.74 (s, 1H), 8.00 – 7.88 (m, 2H), 7.82 – 7.70 (m, 2H), 7.63 – 7.53 (m, 2H), 7.42 – 7.29 (m, 2H), 7.19 – 6.97 (m, 1H) ppm. ^{13}C{^{1}H} NMR (100 MHz, DMSO-d6) δ 167.8, 150.9, 137.6, 131.6, 130.4, 129.0, 127.0, 123.8, 119.8 ppm. IR (Neat) 1693, 1672, 1600, 1565, 1466, 1270, 1228, 1073 cm^{-1}. HRMS (ESI$^+$) m/z: [M + H] calcd $C_{14}H_{12}BrN_2O_2$ for: 319.0082, found: 319.0075.

*4-iodo-N-(phenylcarbamoyl)benzamide (**3ib**)*: white solid, 37 mg, 50%, m. p. = 247-248 °C, ^{1}H NMR (400 MHz, DMSO-d6) δ 11.10 (s, 1H), 10.74 (s, 1H), 8.05 – 7.86 (m, 2H), 7.83 – 7.75 (m, 2H), 7.67 – 7.52 (m, 2H), 7.44 – 7.27 (m, 2H), 7.24 – 6.99 (m, 1H) ppm. ^{13}C{^{1}H} NMR (100 MHz, DMSO-d6) δ 168.2, 150.9, 137.5, 131.8, 130.1, 129.0, 123.8, 119.9, 101.5 ppm. IR (Neat) 1714, 1694, 1644, 1504, 1486, 1470, 1463, 917 cm^{-1}. HRMS (ESI$^+$) m/z: [M + H] calcd $C_{14}H_{12}IN_2O_2$ for: 366.9938, found: 366.9944.

*methyl 4-((phenylcarbamoyl)carbamoyl)benzoate (**3jb**)*: white solid, 54 mg, 90%, m. p. = 208-209 °C, ^{1}H NMR (400 MHz, DMSO-d6) δ 11.21 (s, 1H), 10.70 (s, 1H), 8.15 – 8.01 (m, 4H), 7.61 – 7.50 (m, 2H), 7.41 – 7.32 (m, 2H), 7.16 – 7.06 (m, 1H), 3.90 (s, 3H) ppm. ^{13}C{^{1}H} NMR (100 MHz, DMSO-d6) δ 168.0, 165.5, 150.8, 137.5, 136.4, 133.1, 129.2, 128.7, 127.8, 119.9, 52.6 ppm. IR (Neat) 1721, 1676, 1690, 1491, 1476, 1271, 1226, 1126 cm^{-1}. HRMS (ESI$^+$) m/z: [M + H] calcd $C_{16}H_{15}N_2O_4$ for: 299.1032, found: 299.1021.

*4-cyano-N-(phenylcarbamoyl)benzamide (**3kb**)*[26]: white solid, 52 mg, >98%, m. p. = 208-209 °C, ^{1}H NMR (400 MHz, DMSO-d6) δ 11.26 (s, 1H), 10.64 (s, 1H), 8.20 – 8.09 (m, 2H), 8.08 – 7.96 (m, 2H), 7.67 – 7.51 (m, 2H), 7.36 (t, *J = 7.9* Hz, 2H), 7.12 (t, *J = 7.4* Hz, 1H) ppm. ^{13}C{^{1}H} NMR (100 MHz, DMSO-d6) δ 168.0, 151.2, 137.9, 137.0, 133.0, 129.5, 128.7, 124.4, 120.4, 118.6, 115.5 ppm.

*N-(phenylcarbamoyl)-4-(4,4,5,5-tetramethyl-1,3,2-dioxaborolan-2-yl)benzamide (**3lb**)*: white solid, 48 mg, 65%, m. p. = 218-219 °C, ^{1}H NMR (400 MHz, DMSO-d6) δ 11.10 (s, 1H), 10.76 (s, 1H), 8.01 (d, *J = 8.3* Hz, 2H), 7.80 (d, *J = 8.3* Hz, 2H), 7.59 (dd, *J = 8.6, 1.0* Hz, 2H), 7.42 – 7.33 (m, 2H), 7.15 – 7.07 (m, 1H), 1.32 (s, 12H) ppm. ^{13}C{^{1}H} NMR (100 MHz, DMSO-d6) δ 168.6, 150.9, 137.6, 134.8, 134.3, 129.0, 127.6, 119.8, 104.6, 84.1, 24.7 ppm. IR (Neat) 1696, 1598, 1556, 1487, 1448, 1361, 1264, 1229 cm^{-1}. HRMS (ESI$^+$) m/z: [M + H] calcd $C_{20}H_{24}BN_2O_4$ for: 367.1827, found: 367.1815.

*N-(phenylcarbamoyl)-4-vinylbenzamide (**3mb**)*: white solid, 49 mg, 92%, m. p. = 189-190 °C, ^{1}H NMR (400 MHz, DMSO-d6) δ 11.02 (s, 1H), 10.86 (s, 1H), 8.02 (d, *J = 8.0* Hz, 2H), 7.61 (dd, *J = 16.8, 8.0* Hz, 4H), 7.44 – 7.27 (m, 2H), 7.19 – 7.05 (m, 1H), 6.82 (dd, *J = 17.5*, 11.0 Hz, 1H), 6.03 (d, *J = 17.7* Hz, 1H), 5.43 (d, *J = 10.9* Hz, 1H) ppm. ^{13}C{^{1}H} NMR (100 MHz, DMSO-d6) δ 168.2, 151.1, 141.5, 137.6, 135.7, 131.3, 128.8, 126.2, 123.7, 119.8, 117.4, 104.6 ppm. IR (Neat) 1691, 1602, 1562, 1475, 1362, 1273, 1234, 1185 cm^{-1}. HRMS (ESI$^+$) m/z: [M + H] calcd $C_{16}H_{15}N_2O_2$ for: 267.1134, found: 267.1126.

*N-(phenylcarbamoyl)-2-naphthamide (**3nb**)*[28]: white solid, 57 mg, 98%, m. p. = 193-194 °C, ^{1}H NMR (400 MHz, DMSO-d6) δ 11.18 (s, 1H), 10.89 (s, 1H), 8.73 (s, 1H), 8.26 – 7.95 (m, 4H), 7.83 – 7.53 (m, 4H), 7.49 – 7.27 (m, 2H), 7.23 – 6.96 (m, 1H) ppm. ^{13}C{^{1}H} NMR (100 MHz, DMSO-d6) δ 168.8, 151.2, 137.7, 134.9, 131.9, 129.6, 129.5, 129.3, 129.0, 128.6, 128.3, 127.7, 127.1, 124.2, 123.8, 119.8 ppm.

*2-phenyl-N-(phenylcarbamoyl)acetamide (**3ob**)*[29]: white solid, 45 mg, 88%, m. p. = 154-155 °C, ^{1}H NMR (400 MHz, DMSO-d6) δ 10.94 (s, 1H), 10.46 (s, 1H), 7.57 – 7.40 (m, 2H), 7.40 – 7.23 (m, 7H), 7.13 – 7.03 (m, 1H), 3.72 (s, 2H) ppm. ^{13}C{^{1}H} NMR (100 MHz, DMSO-d6) δ 173.7, 150.8, 137.5, 134.4, 129.5, 129.0, 128.9, 128.4, 126.9, 119.7, 42.5 ppm.

*3-phenyl-N-(phenylcarbamoyl)propanamide (**3pb**)*[30]: white solid, 35 mg, 65%, m. p. = 146-147 °C, ^{1}H NMR (400 MHz, DMSO-d6) δ 10.71 (s, 1H), 10.54 (s, 1H), 7.56 – 7.47 (m, 2H), 7.39 – 7.15 (m, 7H), 7.13 – 7.00 (m, 1H), 2.89 (t, *J* = 7.7 Hz, 2H), 2.71 (t, *J* = 7.7 Hz, 2H) ppm. ^{13}C{^{1}H} NMR (100 MHz, DMSO-d6) δ 174.9, 150.8, 140.5, 137.5, 128.9, 128.4, 128.2, 126.1, 123.7, 119.6, 37.3, 29.9 ppm. IR (Neat) 1687, 1602, 1562, 1499, 1449, 1235, 753, 697 cm^{-1}. HRMS (ESI$^+$) m/z: [M + H] calcd $C_{16}H_{17}N_2O_2$ for: 269.1284, found: 269.1289.

*N-(phenylcarbamoyl)benzo[d][1,3]dioxole-5-carboxamide (**3qb**)*[31]: white solid, 43 mg, 94%, m. p. = 178-180 °C, ^{1}H NMR (400 MHz, DMSO-d6) δ 10.87 (s, 1H), 10.85 (s, 1H), 7.68 (dd, *J = 8.2, 1.9* Hz, 1H), 7.60 – 7.58 (m, 2H), 7.58 – 7.56 (m, 1H), 7.35 (dd, *J = 8.4, 7.5* Hz, 2H), 7.13 – 7.08 (m, 1H), 7.07 (d, *J = 8.2* Hz, 1H), 6.15 (s, 2H) ppm. ^{13}C{^{1}H} NMR (100 MHz, DMSO-d6) δ 167.5, 151.4, 151.2, 147.6, 137.6, 129.0, 125.8, 124.3, 119.8, 108.1, 102.1 ppm.

*N-(phenylcarbamoyl)furan-2-carboxamide (**3rb**)*[31]: white solid, 47 mg, 84%, m. p. = 204-206 °C, ^{1}H NMR (400 MHz, DMSO-d6) δ 10.91 (s, 1H), 10.56 (s, 1H), 8.05 (dd, *J = 1.7, 0.7* Hz, 1H), 7.72 (dd, *J = 3.6, 0.8* Hz, 1H), 7.62 – 7.44 (m, 2H), 7.50 – 7.19 (m, 2H), 7.24 – 6.97 (m, 1H), 6.75 (dd, *J = 3.6, 1.7* Hz, 1H) ppm. ^{13}C{^{1}H} NMR (100 MHz, DMSO-d6) δ 158.5, 150.8, 148.0, 145.1, 137.6, 129.0, 123.7, 119.8, 117.7, 112.5 ppm.

*N-(phenylcarbamoyl)benzofuran-2-carboxamide (**3sb**)*[32]: white solid, 48 mg, 82%, m. p. = 234-236 °C, ^{1}H NMR (400 MHz, DMSO-d6) δ 11.17 (s, 1H), 10.51 (s, 1H), 8.11 (d, *J = 0.9* Hz, 1H), 7.88 – 7.83 (m, 1H), 7.73 (dd, *J = 8.4, 0.8* Hz, 1H), 7.61 – 7.52 (m, 3H), 7.42 – 7.33 (m, 3H), 7.16 – 7.09 (m, 1H) ppm. ^{13}C{^{1}H} NMR (100 MHz, DMSO-d6) δ 159.2, 154.9, 151.5, 150.5, 146.4, 137.5, 129.0, 126.7, 123.5, 123.5, 119.9, 113.2, 112.1 ppm.

*N-(phenylcarbamoyl)thiophene-2-carboxamide (**3tb**)*[33]: white solid, 44 mg, 90%, m. p. = 210-211 °C, ^{1}H NMR (400 MHz, DMSO-d6) δ 11.13 (s, 1H), 10.67 (s, 1H), 8.28 (dd, *J = 3.9, 1.1* Hz, 1H), 8.03 (dd, *J = 5.0, 1.1* Hz, 1H), 7.74 – 7.48 (m, 2H), 7.42 – 7.28 (m, 2H), 7.25 (dd, *J = 5.0, 3.9* Hz, 1H), 7.21 – 7.03 (m, 1H) ppm. ^{13}C{^{1}H} NMR (100 MHz, DMSO-d6) δ 162.8, 150.9, 137.6, 137.2, 134.9, 131.9, 129.0, 128.8, 123.8, 119.9 ppm.

*1-methyl-N-(phenylcarbamoyl)-1H-indole-2-carboxamide (**3ub**)*: white solid, 57 mg, >98%, m. p. = 228-229 °C, ^{1}H NMR (400 MHz, DMSO-d6) δ 11.13 (s, 1H), 10.56 (s, 1H), 8.59 (s, 1H), 8.27 – 8.16 (m, 1H), 7.65 – 7.55 (m, 3H), 7.41 – 7.21 (m, 5H), 7.17 – 7.03 (m, 1H), 3.88 (s, 3H) ppm. ^{13}C{^{1}H} NMR (100 MHz, DMSO-d6) δ 165.6, 151.8, 137.9, 137.1, 135.2, 128.9, 126.8, 123.4, 122.8, 121.9, 121.1, 119.7, 110.9, 106.8, 33.5 ppm. IR (Neat) 1719, 1698, 1596, 1561, 1490, 1260, 1232, 1192 cm^{-1}. HRMS (ESI$^+$) m/z: [M + H] calcd $C_{17}H_{16}N_3O_2$ for: 294.1242, found: 294.1233.

*N-(phenylcarbamoyl)quinoline-6-carboxamide (**3vb**)*: white solid, 55 mg, 94%, m. p. = 184-185 °C, ^{1}H NMR (400 MHz, DMSO-d6) δ 11.24 (s, 1H), 10.81 (s, 1H), 9.06 – 9.01 (m, 1H), 8.77 (d, *J = 1.6* Hz, 1H), 8.52 (d, *J = 8.4* Hz, 1H), 8.27 (dd, *J = 8.9, 2.0* Hz, 1H), 8.14 (d, *J = 8.8* Hz, 1H), 7.66 (dd, *J = 8.3, 4.2* Hz, 1H), 7.61 (d, *J = 7.7* Hz, 2H), 7.42 – 7.31 (m, 2H), 7.21 – 7.09 (m, 1H) ppm. ^{13}C{^{1}H} NMR (100 MHz, DMSO-d6) δ 168.3, 160.4, 152.9, 151.0, 149.2, 137.6, 137.5, 130.1, 130.0, 129.3, 129.0, 127.9, 126.9, 123.8, 122.5, 119.9 ppm. IR (Neat) 1718, 1708, 1675, 1598, 1499, 1281, 1260, 1095 cm^{-1}. HRMS (ESI$^+$) m/z: [M + H] calcd $C_{17}H_{14}N_3O_2$ for: 292.1086, found: 292.1092.

*1,3-diphenylurea (**3wb**)*[5e]: white solid, 40 mg, 94%, m. p. = 238-239 °C, ^{1}H NMR (400 MHz, DMSO-d^6) δ 8.67 (s, 2H), 7.53 – 7.42 (m, 4H), 7.34 – 7.23 (m, 4H), 7.02 – 6.93 (m, 2H) ppm. ^{13}C{^{1}H} NMR (100 MHz, DMSO-d^6) δ 152.6, 139.8, 128.9, 121.9, 118.3 ppm.

*1-benzyl-3-phenylurea (**3xb**)* [5e]: white solid, 16 mg, 36%, m. p. = 169-171 °C, ^{1}H NMR (300 MHz, DMSO-*d*6) δ 8.57 (s, 1H), 7.54 – 7.14 (m, 9H), 6.89 (t, *J* = 7.3 Hz, 1H), 6.62 (t, *J* = 6.0 Hz, 1H), 4.30 (d, *J* = 5.9 Hz, 2H) ppm. ^{13}C{^{1}H} NMR (100 MHz, DMSO-d^6) δ 155.2, 140.5, 140.4, 128.6, 128.3, 127.1, 126.7, 121.1, 117.7, 42.7 ppm.

ASSOCIATED CONTENT

Supporting Information. Examination details of reaction conditions, ^{1}H and ^{13}C NMR spectra for compounds, DFT calculation data and mechanism study details. This material is available free of charge via the Internet at http://pubs.acs.org.

AUTHOR INFORMATION

Corresponding Author

zhangzhh@cau.edu.cn
leijiao@mail.tsinghua.edu.cn

ACKNOWLEDGMENT

This project is supported by National Key Research and Development program of China (2018YFD0200100) and the National Natural Science Foundation of China (No. 21672256). We appreciate Prof. Zhiyuan Zhang and Ms. Huan Sun of National Institute of Biological Sciences (Beijing) for LC-MS analysis support of initial rate kinetics experiments. The Tsinghua Xuetang Talents Program are acknowledged for providing computational resources. We also acknowledge Prof. Haixiang Gao of China Agriculture University, and Dr. Di Qiu of Tianjin Normal University for helpful discussion.

REFERENCES

(1) (a) Karmouta, M. G.; Miocque, M.; Derdour, A.; Gayral, P.; Lafont, O. Synthèse de cyanacétylurées en vue d'essais vis-à-vis d'Hymenolepis nana *Eur. J. Med. Chem*. **1989**, 24, 547; (b) Ranise, A.; Schenone, S.; Bruno, O.; Bondavalli, F.; Filippelli, W.; Falcone, G.; Rivaldi, B. N-Acyl-N-Phenyl Ureas of Piperidine and Substituted Piperidines Endowed with Anti-Inflammatory and Anti-Proliferative Activities. *Il Farmaco* **2001**, *56*, 647.

(2) (a) Stokes, S.; Martin, N. G. A Simple and Efficient Synthesis of N-benzoyl Ureas. *Tetrahedron Lett.* **2012**, *53* (36), 4802. (b) McCoull, W.; Barton, P.; Brown, A. J.; Bowker, S. S.; Cameron, J.; Clarke, D. S.; Davies, R. D.; Dossetter, A. G.; Ertan, A.; Fenwick, M.; Green, C.; Holmes, J. L.; Martin, N.; Masters, D.; Moore, J. E.; Newcombe, N. J.; Newton, C.; Pointon, H.; Robb, G. R.; Sheldon, C.; Stokes, S.; Morgan, D. Identification, Optimization, and Pharmacology of Acylurea GHS-R1a Inverse Agonists. *J. Med. Chem.* **2014**, *57* (14), 6128. (c) Geyer, M.; Baus, J. A.; Fjellstrom, O.; Wellner, E.; Gustafsson, L.; Tacke, R. Synthesis and Pharmacological Properties of Silicon-Containing GPR81 and GPR109A Agonists. *ChemMedChem* **2015**, *10* (12), 2063.

(3) (a) Wiley, P. F. The Reaction of Amides with Isocyanates. *J. Am. Chem. Soc.* **1949**, *71* (4), 1310. (b) Chang, Y. H.; Chiu, F.-T.; Zon, G. Investigation of Thermally Induced α-deoxysilylation of Organosilylated Hydroxylamine Derivatives as a General Method for Nitrene Production. *J. Org. Chem.* **1981**, *46* (2), 342.

(4) (a) *Handbook of Organopalladium Chemistry for Organic Synthesis*; Negishi, E., Ed.; John Wiley&Sons, Inc.: New York, 2002. (b) *Palladium Reagents and Catalysts: New Perspectives for the 21st Century*; Tsuji, J., John Wiley&Sons, Inc., **2004**. (c) Xiao, Q.; Zhang, Y.; Wang, J. Diazo Compounds and N-Tosylhydrazones: Novel Cross-Coupling Partners in Transition-Metal-Catalyzed Reactions *Acc. Chem. Res.* **2013**, *46* (2), 236. (d) Wu, X. -F.; Neumann, H.; Beller, M. Palladium-catalyzed Carbonylative Coupling Reactions between Ar-X and carbon Nucleophiles. *Chem. Soc. Rev.* **2011**, *40* (10), 4986.

(5) (a) Collman, J. P.; Kubota, M.; Hosking, J. W. Hosking Metal Ion Facilitation of Atom-transfer Oxidation-reduction Reactions. *J. Am. Chem. Soc.* **1967**, *89* (18), 4809. (b) Ren, L.; Jiao, N. $PdCl_2$ Catalyzed Efficient Assembly of Organic Azides, CO, and Alcohols under Mild Conditions: A Direct Approach to Synthesize Carbamates. *Chem. Commun.* **2014**, *50* (28), 3706. (c) Chow, S. Y.; Stevens, M. Y.; Odell, L. R. Sulfonyl Azides as Precursors in Ligand-Free Palladium-Catalyzed Synthesis of Sulfonyl Carbamates and Sulfonyl Ureas and Synthesis of Sulfonamides. *J. Org. Chem.* **2016**, *81* (7), 2681. (d) Zhao, J.; Li, Z.; Song, S.; Wang, M. A.; Fu, B.; Zhang, Z. Product-Derived Bimetallic Palladium Complex Catalyzes Direct Carbonylation of Sulfonylazides. *Angew. Chem. Int. Ed.* **2016**, *55* (18), 5545. (e) Zhao, J.; Li, Z.; Yan, S.; Xu, S.; Wang, M. A.; Fu, B.; Zhang, Z. Pd/C Catalyzed Carbonylation of Azides in the Presence of Amines. *Org. Lett.* **2016**, *18* (8), 1736.

(6) Zhang, Z.; Li, Z.; Fu, B.; Zhang, Z. Palladium-catalyzed Cross-coupling Reaction of Azides with Isocyanides. *Chem. Commun.* **2015**, *51* (91), 16312.

(7) Miloserdov, F. M.; Grushin, V. V. Palladium-Catalyzed Aromatic Azidocarbonylation. *Angew. Chem. Int. Ed.* **2012**, 51, 3668.

(8) (a) An example about the kinetic study of azide reaction: Rodionov, V. O.; Fokin, V. V.; Finn, M. G. Mechanism of the Ligand-free CuI-catalyzed Azide-alkyne Cycloaddition Reaction. *Angew. Chem. Int. Ed.* **2005**, *44* (15), 2210; (b) Kinetic study method: Aliquots taken at intervals from the reactions by a microsyringe under insert carbon monoxide atmosphere were quenched with MeOH. Quantitative LC-MS analysis of the resulting samples (VanGuard BEH C18 column, MS detection in single-ion mode) allowed the collection of reliable kinetic data for reactions.

(9) In a high-pressure gas reactor, N_2 was firstly added to 500 psi after degassing, and then CO was added until the pressure of the gas reactor was 1000 psi. The mixture was blended for 24 h, which gave 50% pressure of CO. A balloon with 50% CO content was used in the reaction. In the same way, 40%, 66.7% and 80% CO content balloons was carried out.

(10) (a) Hammett, L. P. The Effect of Structure upon the Reactions of Organic Compounds Benzene Derivatives. *J. Am. Chem. Soc.* **1937**, *59* (1), 96. (b) Jaffé, H. H. A Reëxamination of the Hammett Equation. *Chem. Rev.* **1953**, *53* (2), 191. (c) Brown, H. C.; Okamoto, Y. Electrophilic Substituent Constants. *J. Am. Chem. Soc.* **1958**, *80* (18), 4979.

(11) (a) Li, H.; Dong, K.; Jiao, H.; Neumann, H.; Jackstell, R.; Beller, M. The Scope and Mechanism of Palladium-catalyzed Markovnikov Alkoxycarbonylation of Alkenes. *Nat. Chem.* **2016**, *8* (12), 1159. (b) Willcox, D.; Chappell, B. G. N.; Hogg, K. F.; Calleja, J.; Smalley, A. P.; Gaunt, M. J. A General Catalytic β-C-H Carbonylation of Aliphatic Amines to β-lactams. *Science* **2016**, *354* (6314), 851.

(12) (a) Mindiola, D. J.; Hillhouse, G. L. Terminal Amido and Imido Complexes of Three-Coordinate Nickel. *J. Am. Chem. Soc.* **2001**, *123* (19), 4623. (b) Jenkins, D. M.; Betley, T. A.; Peters, J. C. Oxidative Group Transfer to Co(I) Affords a Terminal Co(III) Imido Complex. *J. Am. Chem. Soc.* **2002**, *124* (38), 11238. (c) Cowley, R. E.; Eckert, N. A.; Elhaïk, J.; Holland, P. L. Catalytic Nitrene Transfer from An Imidoiron(III) Complex to Form Carbodiimides and Isocyanates. *Chem. Commun.* **2009**, (13), 1760. (d) Scepaniak, J. J.; Bontchev, R. P.; Johnson, D. L.; Smith, J. M. Snapshots of Complete Nitrogen Atom Transfer from An Iron(IV) Nitrido Complex. *Angew. Chem. Int. Ed.* **2011**, *50* (29), 6630.

(13) (a) Badiei, Y. M.; Krishnaswamy, A.; Melzer, M. M.; Warren, T. H. Transient Terminal Cu-nitrene Intermediates from Discrete Dicopper Nitrenes. *J. Am. Chem. Soc.* **2006**, *128* (47), 15056. (b) Laskowski, C. A.; Hillhouse, G. L. Group-Transfer Reactions of Ni(II)−Ni(II) Bridging Imido Complexes. Catalytic Formation of Carbodiimides and Isocyanates *via* Nitrene Transfer from Organoazides. *Organometallics* **2009**, *28* (20), 6114.

(14) (a) Cenini, S.; Gallo, E.; Caselli, A.; Ragaini, F.; Fantauzzi, S.; Piangiolino, C. Coordination Chemistry of Organic Azides and Amination Reactions Catalyzed by Transition Metal Complexes. *Coord. Chem. Rev.* **2006**, *250* (11-12), 1234. (b) D'Errico, J. J.; Messerle, L.; Curtis, M. D. Metal-metal Multiple Bonds. 13. Structural Diversity in the Reactions of $Cp_2Mo_2(CO)_4$(Mo≡Mo) with Diazoalkanes and Aryl Azides. *Inorg. Chem.* **1983**, *22* (5), 849. (c) Williams, G. D.; Geoffroy, G. L.; Rheingold, A. L. Reaction of (η^5-MeC_5H_4)$Mn(CO)_2$(THF) with $PhCH_2N_3$ to Yield Binuclear (η^5-

$MeC_5H_4)_2Mn_2(CO)_3[\mu$-$CON(CH_2Ph)N_2]$, An Intermediate in the Formation of Benzyl Isocyanate. *Organometallics* **1986**, *5* (5), 894.

(15) (a) Besenyei, G.; Párkányi, L.; Foch, I.; Simándi, L. I.; Kálmán, A. Insertion of Arylsulfonylnitrene Fragments into Pd–Pd bonds. Crystallographic Characterization of the Novel $[Pd_2Cl_2(\mu$-dppm$)_2(\mu$-$NSO_2\ C_6H_4NO_2$-2)] A-frame Adduct. *Chem. Commun.* **1997**, (12), 1143. (b) Besenyei, G.; Párkányi, L.; Szalontai, G.; Holly, S.; Pápai, I.; Keresztury, G.; Nagy, A. N-benzoylimido Complexes of Palladium. Synthesis, Structural Characterisation and Structure-reactivity Relationship. *Dalton Trans.* **2004**, (13), 2041.

(16) (a) Harrison, J. G.; Gutierrez, O.; Jana, N.; Driver, T. G.; Tantillo, D. J. Mechanism of Rh_2(II)-Catalyzed Indole Formation: The Catalyst Does Not Control Product Selectivity. *J. Am. Chem. Soc.* **2016**, *138* (2), 487. (b) Park, S. H.; Kwak, J.; Shin, K.; Ryu, J.; Park, Y.; Chang, S. Mechanistic Studies of the Rhodium-catalyzed Direct C-H Amination Reaction Using Azides as the Nitrogen Source. *J. Am. Chem. Soc.* **2014**, *136* (6), 2492.

(17) This carbonylation reaction of acyl azides has been carried out with stoichiometric palladium complexes in different conditions. Unfortunately, no palladium intermediate could be detected. This extremely low barrier is the reason.

(18) Xiao, X.; Hou, C.; Zhang, Z.; Ke, Z.; Lan, J.; Jiang, H.; Zeng, W. Iridium(III)-Catalyzed Regioselective Intermolecular Unactivated Secondary Csp(3) -H Bond Amidation. *Angew. Chem. Int. Ed.* **2016**, *55* (39), 11897.

(19) Yang, G.; Chen, Z.; Zhang, H. Clean Synthesis of An Array of N-benzoyl–N′-aryl Ureas Using Polymer-supported Reagents. *Green Chem.* **2003**, *5* (4), 441.

(20) Stokes, S.; Martin, N. G. A Simple and Efficient Synthesis of N-benzoyl Ureas. *Tetrahedron Lett.* **2012**, *53* (36), 4802.

(21) Howbert, J. J.; Grossman, C. S.; Crowell, T. A.; Rieder, B. J.; Harper, R. W.; Kramer, K. E.; Tao, E. V.; Aikins, J.; Poore, G. A. Novel Agents Effective against Solid Tumors: the Diarylsulfonylureas. Synthesis, Activities, and Analysis of Quantitative Structure-activity Relationships. *J. Med. Chem.* **1990**, *33* (9), 2393.

(22) Abrahart, E. N. 83. Some Symmetrical Acylarylureas. *J. Chem. Soc.* **1938**, *0*, 424.

(23) H Hacker, H. G.; Meusel, M.; Aschfalk, M.; Gutschow, M. Solid-phase Synthesis of Disubstituted N-acylureas from Resin-bound Ureas and Acyl Chlorides. *ACS Comb. Sci.* **2011**, *13* (1), 59.

(24) Hokfelt, B.; Jonsson, A. Hypoglycemic Activity in Relation to Chemical Structure of Potential Oral Antidiabetic Substances. I. 1-Sulfonyl-3-alkylureas. *J. Med. Pharm. Chem.* **1962**, *5* (2), 231.

(25) Beasley, M. Y.; Petrow, V.; Stephenson, O. Some 1-alkyl-3-aroyl Ureas. *J. Pharm. Pharmacol.* **1961**, *13* (1), 694.

(26) Bjerglund, K.; Lindhardt, A. T.; Skrydstrup, T. Palladium-catalyzed N-acylation of Monosubstituted Ureas Using Near-stoichiometric Carbon Monoxide. *J. Org. Chem.* **2012**, *77* (8), 3793.

(27) Seiller, B.; Heins, D.; Bruneau, C.; Dixneuf, P. H. Efficient Preparations of Acylamides, Acylcarbamates and Acylureas from Alk-1-en-2-yl Esters. *Tetrahedron* **1995**, *51* (40), 10901.

(28) Kutschy, P.; Dzurilla, M.; Ficeri, V.; Koščík, D. New Synthesis of N-Acylurea Derivatives. *Collect. Czech. Chem. Commun.* **1993**, *58* (3), 575.

(29) Sheehan, J. C.; Johnson, D. A. The Synthesis and Reactions of N-acyl Thiol Amino Acids *J. Am. Chem. Soc.* **1952**, *74* (18), 4726.

(30) Laborde, E.; Robinson, L.; Meng, F.; Peterson, B. T.; Villar, H. O.; Anuskiewicz, S. E.; Ishiwata, Y.; Yokochi, S.; Matsumoto, Y.; Kakigami, T.; Inagaki, H.; Jomori, T.; Matsushima, K.; (Telik, Inc., USA; Sanwa Kaguku Kenkyusho Co., Ltd.). Application: WO 2002081463

(31) Deng, M. -Z.; Caubere, P.; Senet, J. P.; Lecolier, S. Condensation of Acyl Chloride on Sodium Cyanate: Preparation of Acyl Isocyanates. *Tetrahedron* **1988**, *44* (19), 6079.

(32) Wang, X.; Song, A.; Zhu, J.; Yang, Z.; Zhang, Z. Hydrogen Peroxide–Promoted Transformation of Thioureas/Thiosemicarbazides to Related Ureas/Semicarbazides at Room Temperature via Grinding. *Synth. Commun.* **2007**, *37* (10), 1627.

(33) Papadopoulos, E. P. Preparation and Reactions of N-ethoxycarbonylthiophene-2-carboxamide and N-ethoxycarbonylthiophene-2-thiocarboxamide *J. Org. Chem.* ***1974****, 39, 2540.*